

Fractional-submerged membrane distillation crystallizer (F-SMDC) for treatment of high salinity solution

Youngkwon Choi^a, Gayathri Naidu^a, Sanghyun Jeong^b, Sangho Lee^c, Saravanamuthu Vigneswaran^{a,*}

^a Faculty of Engineering, University of Technology Sydney (UTS), P.O Box 123, Broadway, NSW 2007 Australia,

^b Graduate School of Water Resources, Sungkyunkwan University (SKKU), 2066, Seobu-ro, Jangan-gu, Suwon-si, Gyeonggi-do, 16419, Republic of Korea,

^c School of Civil and Environmental Engineering, Kookmin University, Seoul 136-702, Republic of Korea

*Corresponding author: Tel +61-2-9514-2641; Fax +61-2-9514-2633; Email: Saravanamuth.Vigneswaran@uts.edu.au

Abstract

Membrane distillation with crystallization (MDC) is an attractive process for high saline seawater reverse osmosis (SWRO) brine treatment. MDC produces additional fresh water while simultaneously recovering valuable resources. This study developed a novel approach of fractional-submerged MDC (F-SMDC) process, in which MD and crystallizer are integrated in a feed tank with a submerged membrane. F-SMDC principle is based on the presence of temperature/concentration gradient (TG/CG) in the feed reactor. The operational conditions at the top portion of the feed reactor (higher temperature and lower feed concentration) was well suited for MD operation, while the bottom portion of the reactor (lower temperature and higher concentration) was favourable for crystal growth. F-SMDC performance with direct contact MD to treat brine and produce sodium sulfate (Na_2SO_4) crystals using TG/CG showed positive results. The TG/CG approach in F-SMDC enabled to achieve higher water recovery for brine treatment with a volume concentration factor

23 (VCF) of over 3.5 compared to VCF of 2.9 with a conventional S-MDC set-up. Further, the high
24 feed concentration and low temperature at the reactor bottom in F-SMDC enabled the formation of
25 Na_2SO_4 crystals with narrow crystal size distribution.

26 **Keywords:** Concentration and temperature gradients; Membrane distillation with fractional
27 crystallization; Resource recovery; Seawater reverse osmosis brine; Sodium sulfate crystal

29 **1. Introduction**

30 Reverse osmosis (RO) based seawater desalination (i.e. SWRO) technology has been widely
31 used to solve global water crisis of fresh water shortage owing to its affordable operation cost and
32 reliability [1-3]. However, one of the major limitations of SWRO is its low recovery (30~50%),
33 resulting in the production of a substantially large amount of concentrated brine that has to be
34 managed [4-6]. The SWRO brine management incurs an additional operating cost to the plant as
35 well as environmental issues when SWRO brine is discharged directly into the environment [7].
36 SWRO brine contains a variety of chemicals (coagulant, chemical washing agent, and pH adjusting
37 agent) which are employed during SWRO process, Also, SWRO brine contains a high concentration
38 of organic and inorganic matters [8-11]. In recent times, simultaneous brine treatment with
39 extraction/production of valuable resources is favoured to offset the treatment cost rather than the
40 approach of treatment followed by disposal. The former is also preferred as give than seawater and
41 likewise seawater brine contains a number valuable elements [12, 13].

42 In this regard, membrane distillation with crystallizer (MDC) shows promising potential in
43 SWRO brine treatment [14-18]. MDC is an integrated process that can achieve high quality fresh
44 water while simultaneously extracting valuable resources from high salinity solution [14]. MDC is
45 attractive compared to traditional crystallization processes because of the following factors: well-
46 controlled saturation rate, faster nucleation rate and reduction of induction time [19]. Moreover, the
47 ability to concentrate solution up to a saturation point with minimal flux decline is an added
48 advantage of MDC [20-22]. Cooling crystallization method is widely used in separation processes
49 for solution having different solubility at different temperatures due to its ease of control and
50 maintenance [23]. However, one of the major limitations is the significant energy consumption due
51 to initial heating (thermal MD operation) followed by cooling for the crystallization.

52 A number of methods such as submerged MD (SMD) have been evaluated in terms of energy
53 consumption and economic benefits to improve the efficiency of conventional MDC process [3, 24,
54 25]. For instance, in SMD process, channelling heated feed solution through a pump to the
55 membrane module can be eliminated, which results in lower heat losses through the feed channel
56 [14, 26]. In this case, the feed tank can also act as a crystallizer, achieving an integrated system [3].
57 Nevertheless, several limitations are still present such as challenging saturated feed concentration
58 effect, and fouling caused by crystal formation in the feed tank as well as on the membrane [27-29].
59 Previous studies have shown that at elevated feed concentration levels [3], MD performance is
60 affected by flux decline and wetting phenomenon. This decreases the membrane life span, resulting
61 in more frequent membrane replacement, incurring addition operation cost [30].

62 In view of this, fractional submerged MDC (F-SMDC) based on principle of maintaining a
63 feed concentration gradient (CG) and feed temperature gradient (TG) in the reactor was evaluated in
64 this study. Maintaining CG and TG in the feed reactor can positively influence both MD and
65 crystallization. CG and TG in the reactor enables to reduce feed concentration and increase feed
66 temperature at the top portion of the reactor where the submerged membrane is located.
67 Simultaneously, the bottom portion of the reactor maintains high feed concentration with low feed
68 temperature which enhances crystallization at the bottom portion of the reactor. This is due to the
69 formation of high saturation state at the bottom portion of the reactor where crystals form
70 continuously during F-SMDC operation. This setting potentially promises higher water recovery,
71 with reduced membrane scaling issues. Further, the continuous extraction of crystal from the bottom
72 of the reactor is expected to reduce the salt contents in feed solution [14].

73 In this study, the feasibility of F-SMDC for the treatment of highly concentrated and saline
74 feed solution was investigated and compared with conventional submerged membrane distillation
75 crystallization (SMDC). The trend of CG/TG in the feed reactor was examined during the operation.

76 The effect on the flux and crystallization efficiency in the F-SMDC was evaluated. In addition,
77 methods to improve the efficiency of maintaining CG/TG in the feed reactor were investigated.

78

79 **2. Materials and Methods**

80 **2.1 Lab-scale setup**

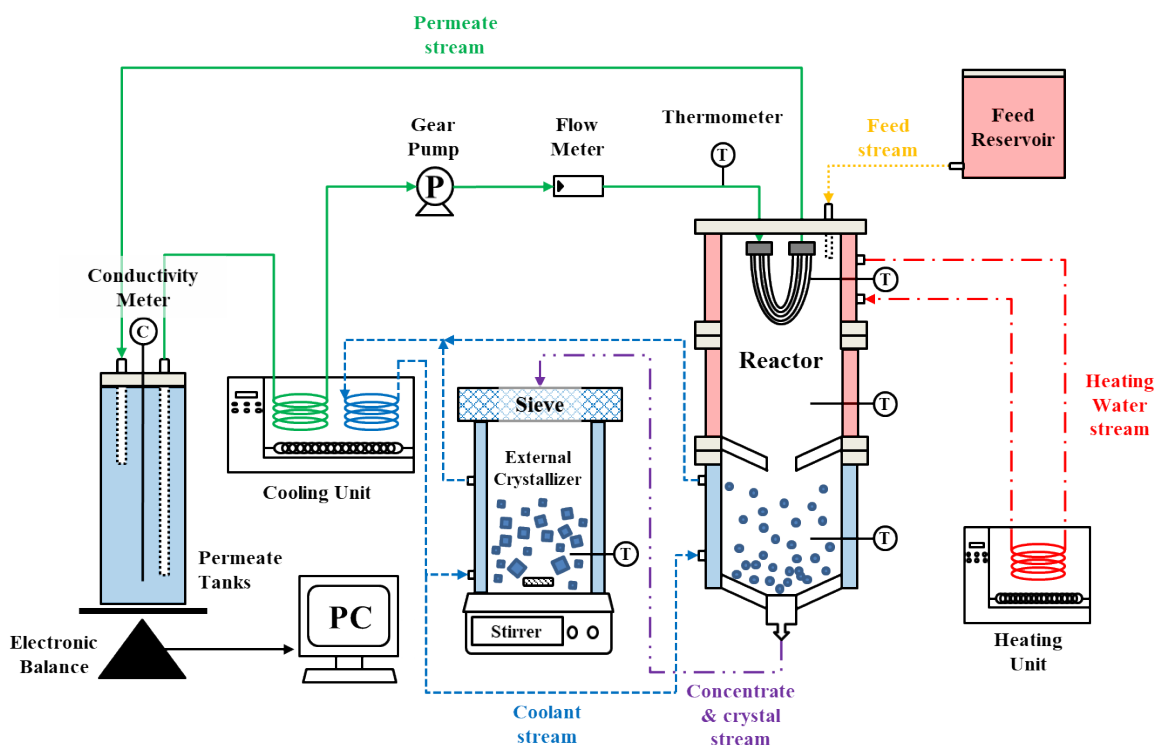
81 F-SMDC process with direct contact MD (DCMD) configuration based on GC and TG was
82 used in this study (**Figure 1**). The F-SMDC reactor consisted of three cylindrical cells with a height
83 of 150 mm and an inner diameter of 70 mm (volume of the single cell = 580 mL, and total volume of
84 the reactor = 1,740 mL). The reactor is equipped with double wall to enable the control of TG as
85 temperature control of feed solution is essential in the reactor (**Figure 2**). The partition in the shape
86 of funnel (length = 25 mm, and hole diameter = 20 mm) was installed between the top and bottom
87 portion. This partition acts as a barrier that minimized the mixing of solution by natural convection
88 caused by heating or cooling. Feed solution was placed inside of the reactor while heating and
89 cooling water was circulated at the outer wall of the reactor with respective heating and cooling
90 units. This enabled the feed solution at the top portion of the reactor to be maintained at 50.0 ± 1.3 °C,
91 while, the feed solution at the bottom portion of the reactor was maintained at 20.0 ± 1.5 °C.
92 Thermometer was placed in each cell to measure the temperature of feed solution in real-time.

93 Meanwhile, the permeate temperature (T_p) was maintained at 16.5 ± 0.2 °C, and was measured
94 using temperature sensors placed at the permeate channel. The permeate flow rate of 0.5 L/min was
95 controlled using a gear-pump. Feed solution was fed continuously into the top portion of the reactor
96 by the differential head of water between the reactor and feed tank. Continuous flow of new feed
97 solution to the top portion of reactor enables to maintain a constant feed solution concentration rather
98 than an increasing feed concentration. This systematically minimizes the effect of increased feed

99 concentration on MD performance. The temperature of feed solution in the feed tank (reservoir) was
100 maintained at room temperature (23.2 ± 0.3 °C).

101 An external crystallizer was used in the last stage of the F-SMDC operation. Upon attaining
102 super-saturation state at the bottom portion of the reactor, the remaining feed solution (mother liquid)
103 was fed to this external reactor. The external reactor was kept at room temperature (23.2 ± 0.3 °C)
104 with constant stirring (50 rpm) of the mother liquid to enhance crystal growth.

105 The permeate flux was calculated from on the solution mass difference with time using an
106 electronic balance. The permeate/fresh water quality was evaluated by measuring the
107 conductivity/total dissolved solids (TDS) value in real-time. All the experiments were duplicated to
108 ensure the reproducibility.

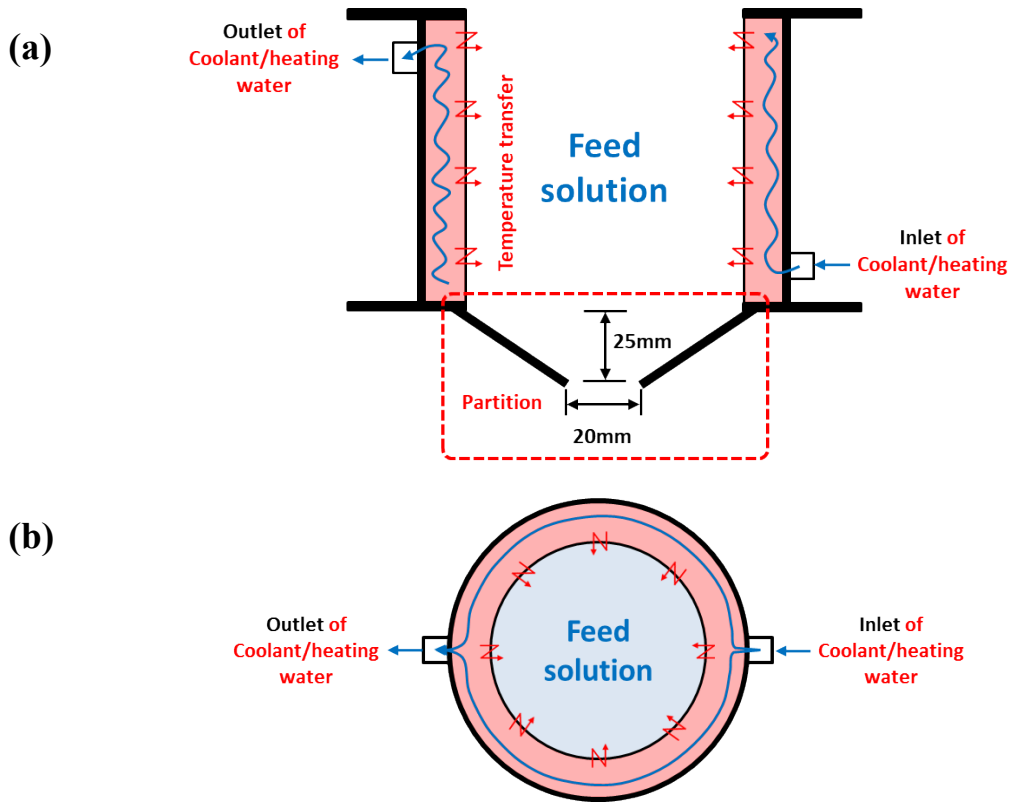


109

110 **Figure 1** Set-up of F-SMDC process: permeate stream (—), stream of continuous feeding to the
111 reactor (feed solution) (·····), stream of concentrate and crystal generated from the reactor to the crystal

112 growth cell (---), the stream of heating water for the top portion of the reactor (---), stream of coolant water
113 for the bottom portion of the reactor and the crystal growth cell (—).

114



115 **Figure 2** Details of F-SMDC reactor showing the double wall feature for generating FT gradient
116 (heating in the top portion of the reactor and cooling at the bottom portion of the reactor): (a) Cross-sectional
117 view, and (b) Aerial view.

118

119 2.2 Feed solution

120 The performance of F-SMDC process was investigated using 120 g/L Na_2SO_4 solution as
121 feed solution. The solubility of Na_2SO_4 in water varies significantly at different temperature (91 g/L
122 @ 10 °C, 195 g/L @ 20 °C, and 488 g/L @ 40 °C). A mixed solution containing sodium chloride

123 (NaCl) and Na₂SO₄ was then used to examine an effect of salinity on treatment of high concentration
124 Na₂SO₄ solution (

125 **Table 1**). Both feed solutions were prepared using reagent grade salts (Sigma-Aldrich).

126

127 **Table 1** Composition of model solution.

Ions	Concentration (mg/L)
Sodium (Na ⁺)	58,320
Sulfate (SO ₄ ²⁻)	81,150
Chloride (Cl ⁻)	30,020

128

129 **2.3 Membrane**

130 A hollow-fiber polyvinylidene fluoride (PVDF) membrane (Econity, Republic of Korea)
131 module was used. The membrane has a nominal pore size of 0.1 μm with an outer and inner diameter
132 of 1.2 mm and 0.7 mm (membrane wall thickness: 250mm), liquid entry pressure (LEP) of 2.0-2.3
133 bar, and contact angle of 106±2° (based on the specifications provided by the manufacturer). A
134 membrane module with an effective membrane area of 0.0136 m² was used. The membrane module
135 consisted of 18 fibers, each of 0.2 m in length, which were potted on both ends of membrane fiber.

136

137 **2.4 Analysis**

138 Crystal morphology was characterized by a field emission scanning electron microscopy
139 (FESEM, Zeiss supra 55VP, Carl Zeiss AG). The TDS and conductivity of the permeate were
140 measured with a portable water quality meter (HQ40d multi, Hach). The concentrated feed solution
141 was measured using calibrated conductivity curves made using different concentration of Na₂SO₄

142 (15, 30, 60, 180 and 300 g/L Na₂SO₄). The concentrated solution was vacuum filtered using a glass
143 microfiber filter (Whatman, Grade GF/C, pore = 1.2 μm) enabling the crystals in the solution to be
144 retained on the filter. The crystals were dried at room temperature (23.2±0.3 °C) for 120 h and the
145 dry weight of crystals was measured using an electronic balance. The crystal form and sizes were
146 evaluated using a microscopy method. In this method, at least 72 crystals were selected randomly,
147 and each crystal was measured using microscope with an image analyser (ImagePro7). The crystal
148 sizes were then quantified with a crystal size distribution (CSD) procedure.

149 Volume concentration factor (VCF) used in this study was based on the reactor volume and
150 the amount of produced fresh water. The total volume of feed solution in F-SMDC reactor was
151 maintained at a fixed volume (1,740 mL) with continuous feeding of feed solution at the same rate of
152 produced fresh water. If the rejection ratio of produced fresh water is 100% over time, the feed
153 solution concentration in the reactor would increase while the total volume of feed solution was
154 maintained. In this context, the VCF value was calculated as:

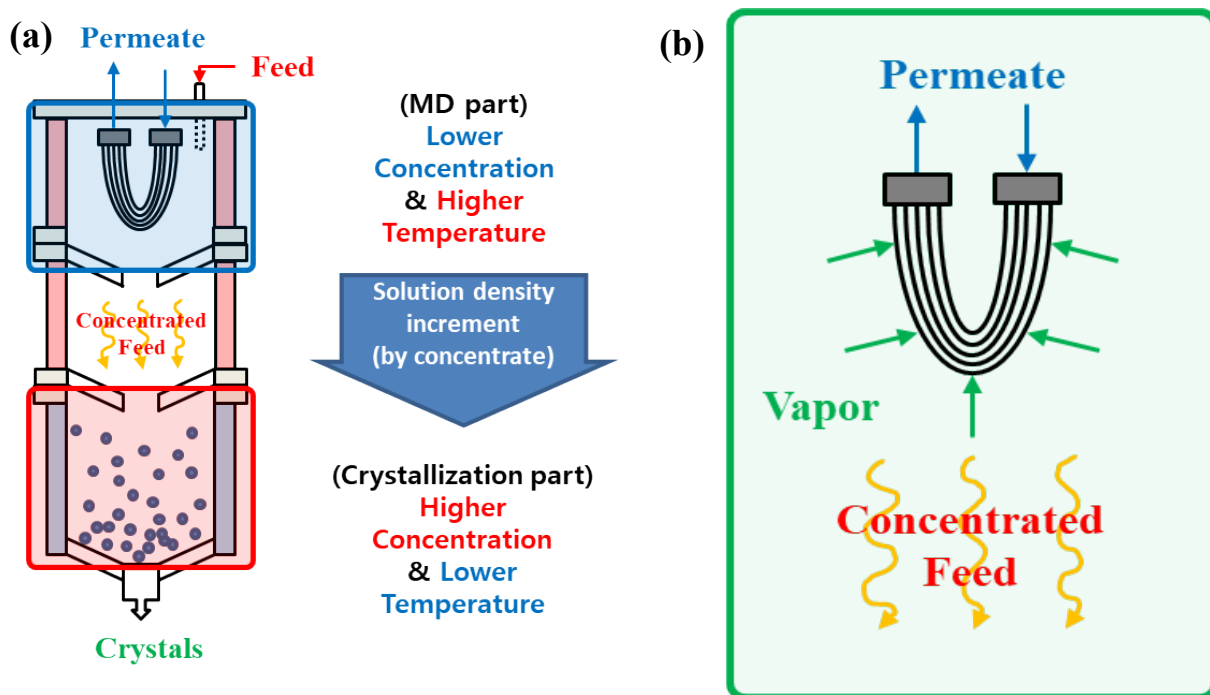
$$VCF = \frac{V_{reactor} + V_{total, permeate}}{V_{reactor}}$$

156 where $V_{reactor}$ is the reactor volume, and $V_{total,permeate}$ is the total amount of permeate produced.

157 3. F-SMDC principle

158 F-SMDC is a combination of two processes: MD and crystallization in a single feed reactor
159 with a submerged membrane (**Figure 3(a)**). The submerged membrane module is placed at the top
160 portion of the feed reactor. In F-SMDC, a CG is generated in the feed reactor as a result of difference
161 in solution density. Upon the increase of feed solution concentration (MD part), the density of the
162 feed solution increases, resulting in the gravitation of concentrated feed solution to the bottom of the
163 reactor (**Figure 3(b)**). In S-DCMD, cooling down of feed solution by the cold permeate stream

164 further enhances this factor as water density is higher at low temperature. Accordingly, CG is
 165 generated in the reactor. Simultaneously, TG is generated by external heating and cooling of the
 166 outer wall (Figure 2).



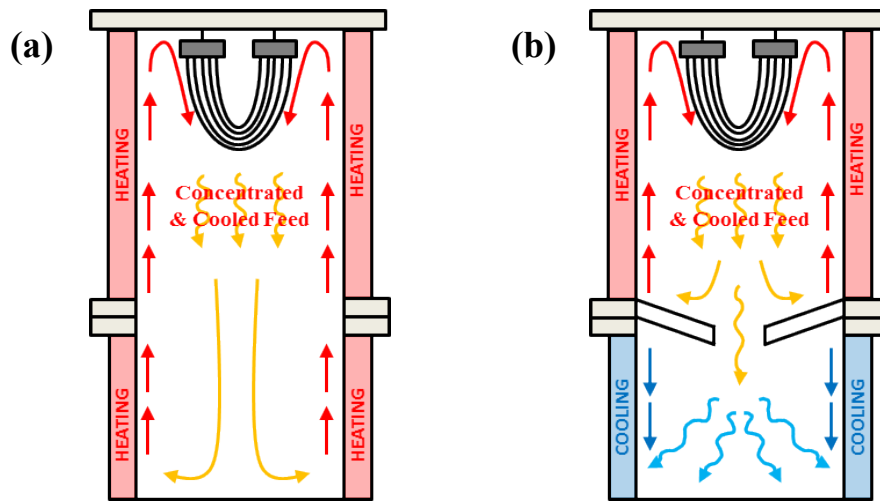
167 **Figure 3** Generation of concentration gradient (CG) in feed reactor of F-SMDC: (a) lower feed
 168 concentration at the top portion and higher feed concentration at the bottom portion, and (b) concentration
 169 effect at the top portion of the reactor containing submerged membrane.

170

171 The presence of CG in the feed reactor influences both MD and crystallization efficiency of
 172 the F-SMDC process. In MD, dissolved ion concentration in the feed solution is increased as the feed
 173 solution is concentrated, resulting in decrease of permeate flux. However, in crystallization process,
 174 elevated dissolved ion contents are favourable for attaining saturation degree of targeted compounds.
 175 Lower concentration at the top portion of the reactor is suitable for MD operation. Higher
 176 concentration at the bottom portion of the reactor is favourable for the formation of crystals since
 177 super-saturation (above the limits of metastable zone) of target salt should be reached to get a

178 nucleation of crystals. F-SMDC achieves an increase of feed concentration at the bottom portion of
179 the reactor at a faster ratio compared with theoretical concentration ratio in the whole reactor, and
180 crystals are formed when solution concentration exceeds the limits of metastable zone of solution.
181 Moreover, TG is formed in the reactor by the temperature transfer caused by movement of
182 concentrated feed solution to the bottom portion without additional temperature control (using
183 heating or cooling). Temperature at the top portion is higher than the bottom portion. The
184 maintenance of TG in F-SMDC enhances the crystallization phenomenon.

185 Convection current in the reactor occurs differently (**Figure 4(a)**). If feed solution is heated
186 up near the reactor wall, its density decreases with its expansion. As a result, it moves towards the
187 upper portion, and the unheated feed solution moves downwards. Moreover, concentrated and cooled
188 (because of the effect of lower permeate temperature (around 16.5 ± 0.2 °C) of S-DCMD) feed
189 solution by membrane operation favours the above effect. As a result, feed solution is mixed, and
190 therefore CG cannot be maintained in the feed reactor. Even though convection current effect on
191 solution mixing does not significantly affect CG, it should still be controlled to ensure that CG is
192 well controlled/maintained throughout the operation. In our design of F-SMDC, the incorporation of
193 a partition in the feed reactor enables to maintain convection current effect within the respective cells
194 (top and bottom portion of the reactor) (**Figure 4(b)**). The partition prevented the feed solution
195 mixing by convection current, resulting in maintaining CG and TG in the reactor.



196 **Figure 4** Convection current in reactor by heating and cooling of (a) conventional MDC process
 197 (reactor without cooling and partition) and (b) F-SMDC process (reactor with cooling and partition).

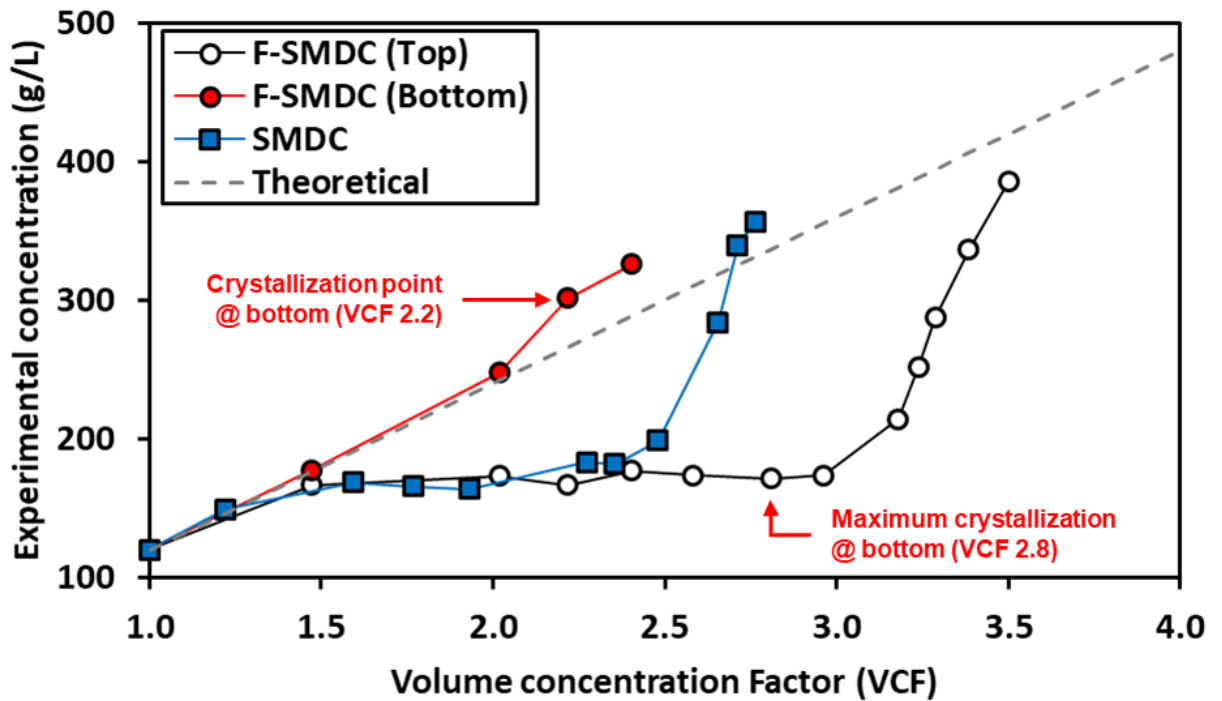
199 4. Results and discussions

200 In this study, the feasibility of F-SMDC was examined for the treatment of feed solution
201 containing Na₂SO₄ alone and with NaCl.

202 4.1. Performance comparison of F-SMDC and SMDC

203 The performance of conventional submerged MDC (SMDC) (reactor without cooling and
204 partitioning) was compared with F-SMDC (reactor with cooling and partitioning) under the same
205 operating conditions (reactor, feed temperature and feed solution) and same sampling points at the
206 top and bottom portion of the reactor. The initial flux of both SMDC and F-SMDC mode was 2.8 and
207 2.7 LMH respectively. The initial flux of S-MDC was slightly higher than F-SMDC, while the feed
208 solution concentration trend varied. Up to a feed solution VCF 2.5, a similar concentration variation
209 was observed for both SMDC and F-SMDC mode. However, in SMDC, above VCF 2.5, a rapid
210 increase of concentration from VCF 2.5 to 2.8 accompanied by a rapid flux decline was observed
211 (Figures 5 and 6). Both processes maintained 99% ion rejection ratio until the end of the experiment.
212 Comparatively, F-SMDC was able to maintain a stable concentrate (without rapid increase) up to
213 VCF 3.0 and sustained the operation up to VCF 3.5. The results indicated that in F-SMDC, the
214 partition between the top and the bottom portion of the reactor prevented the mixing of feed solution
215 by natural convection current, emulating a trap. This enabled to create a CG in the reactor, with a
216 higher concentration at the bottom portion of the reactor. In F-SMDC, the presence of CG in the feed
217 reactor was beneficial for both the MD and crystallization processes. Maintaining a low feed
218 concentration closer to the membrane in F-SMDC enabled to achieve a higher VCF (around VCF
219 3.5) with smaller flux decline compared to the SMDC (around VCF 2.8). In SMDC, concentrated
220 feed solution interferes with the transportation of vapour through the hydrophobic membrane,
221 decreasing its performance (reduced flux decline).

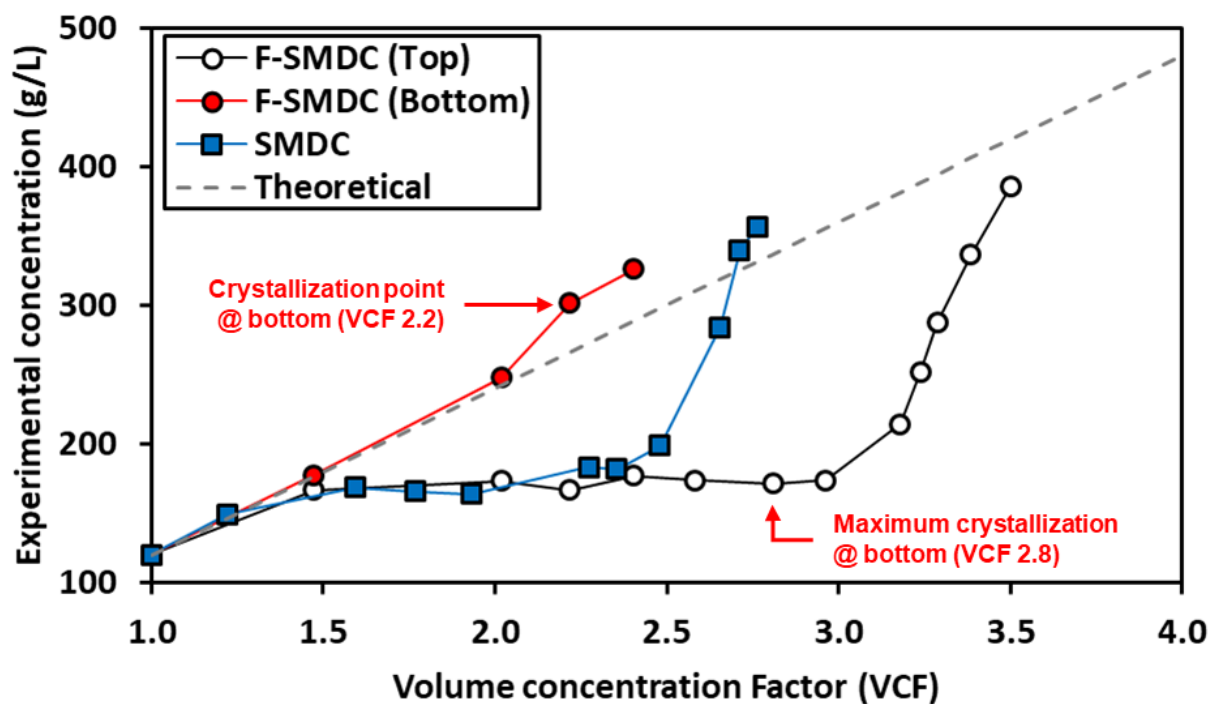
222 In F-SMDC, the presence of CG in the feed reactor was well reflected by the CG variation
223 between the top and bottom portion of the reactor (



224

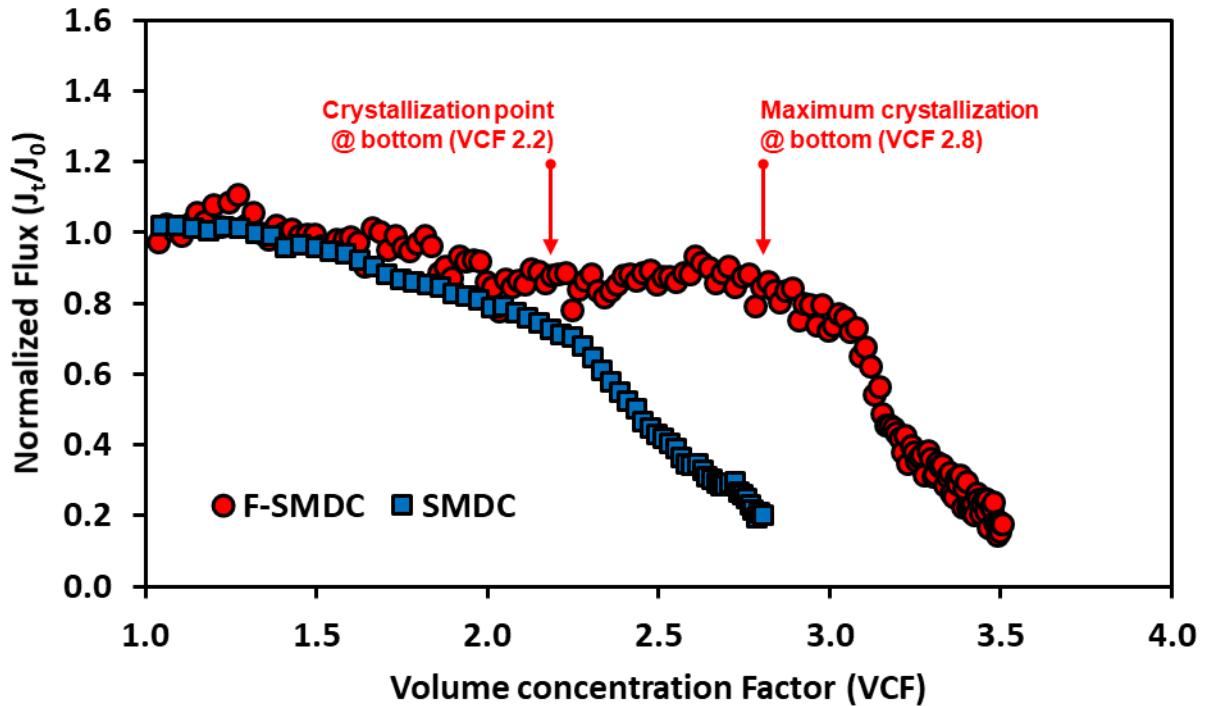
225 **Figure 5).** The CG effect was especially apparent from VCF 1.5 onwards. The feed
226 concentration at the top portion (MD part) of the reactor did not change rapidly while a rapid
227 increase of feed concentration at the bottom portion of the reactor was observed. At the top portion,
228 the feed solution concentration was maintained (range: 171.8 ± 5.1 g/L, 1.4 times of initial feed
229 concentration) below the theoretical feed concentration increment (initial feed concentration \times VCF).
230 Above VCF 2.0, feed concentration at the bottom portion of the reactor showed higher increment
231 than the theoretical feed concentration level. Over time, the feed concentration at the bottom portion
232 of the reactor greatly varied to the theoretical feed concentration. The results reflected the capacity of
233 F-SMDC to maintain a stable CG in the feed reactor.

234 In the F-SMDC mode, higher feed concentration at the bottom portion of the reactor than the
 235 top portion made it suitable for the formation of target crystals. Also, lower temperature (around 20.0
 236 ± 1.5 °C) at the bottom portion of the reactor, which was generated by the cooling as well as the
 237 movement of concentrated/cooled feed solution from the top portion (heated up) was favourable for
 238 the stimulation of crystals.



239

240 **Figure 5** Variation of feed concentration in the reactor during the operation in F-SMDC and SMDC
 241 modes (feed: Na₂SO₄).



242

243

Figure 6 Comparison of flux in F-SMDC and SMDC mode (without crystal extraction).

244

245

246

247

248

249

250

251

252

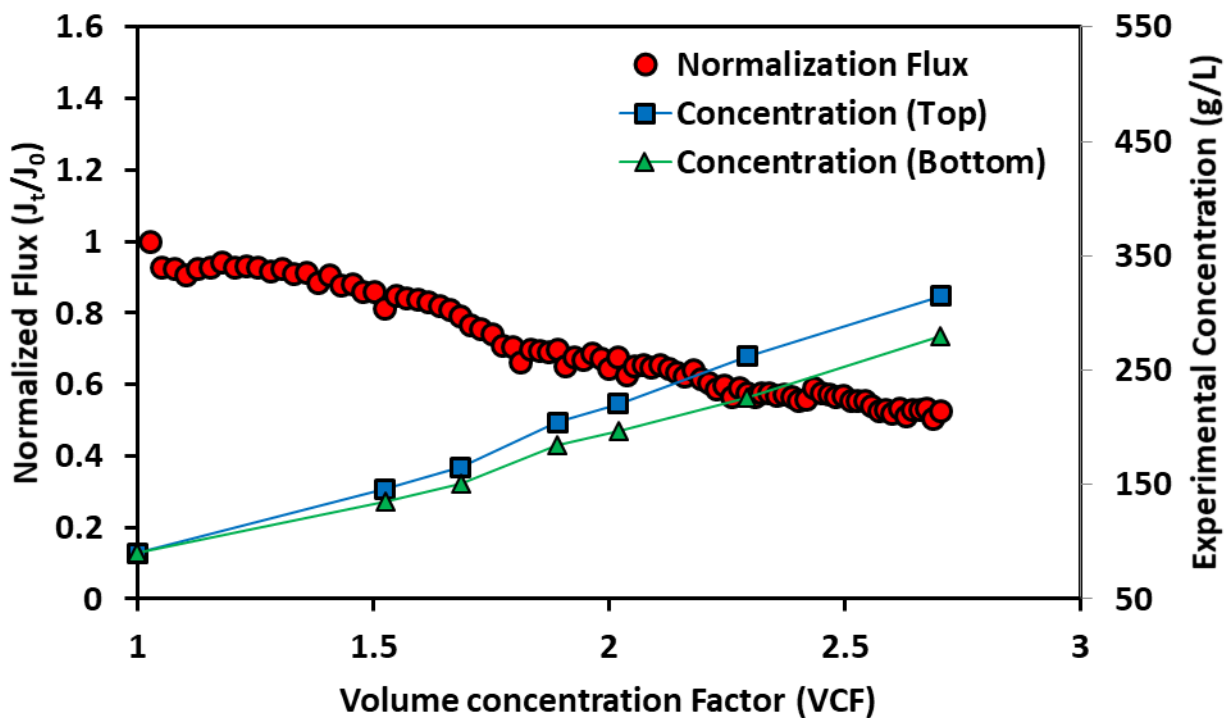
253

254

255

The F-SMDC was carried out using S-DCMD configuration. The feasibility of different submerged MD configurations (submerged vacuum direct contact MD called as S-VDCMD) in F-SMDC process was examined under the same operational condition. The motivation for using S-VDCMD is the potential of achieving higher permeate flux. In line with this, S-VDCMD achieved a 25% higher initial permeate flux than S-DCMD. However, the CG in F-SMDC with S-VDCMD configuration was not observed. Higher flux decline was also observed with S-VDCMD compared to F-SMDC with S-DCMD configuration (Figure 7) with slightly lower feed concentration at the bottom portion than at the top portion of the reactor. This was attributed to the application of vacuum. In a previous S-MD study [3], it was found that the deposition and adhesion of crystals on the membrane surface was intensified by the presence of vacuum pressure in the MD, resulting in more prevalent fouling. In S-VDCMD, concentrated ions were captured in the membrane boundary

256 layer due to stronger driving force (vacuum pressure) compared to S-DCMD [3]. This restricted the
 257 movement of concentrated feed solution, and it stagnated close to the membrane surface. The
 258 increase in diffusion potential of concentrated feed solution at the top portion rather than the
 259 precipitation downward, resulted in the formation of higher concentration at the top portion than the
 260 bottom portion of the reactor. The results highlighted that S-MD using vacuum was not suitable for
 261 F-SMDC process.



262

263 **Figure 7** Normalized flux and concentration tendency in F-SMDC comparing with S-VDCMD.

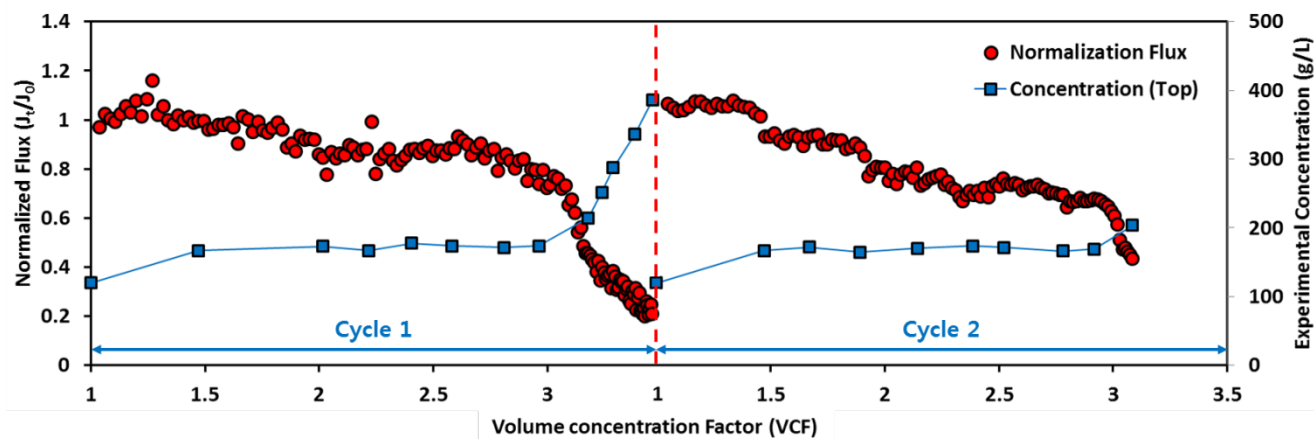
264

265 4.2. Continuous F-SMDC operation

266 The stability of F-SMDC in treating high concentration solution was examined by carrying
 267 out two repeated cycles of operation using the same membrane. At the end of each cycle, used
 268 membrane was submerged in DI water and stirred at 200 rpm for 10 mins to rinse/clean the
 269 membrane before the subsequent operation.

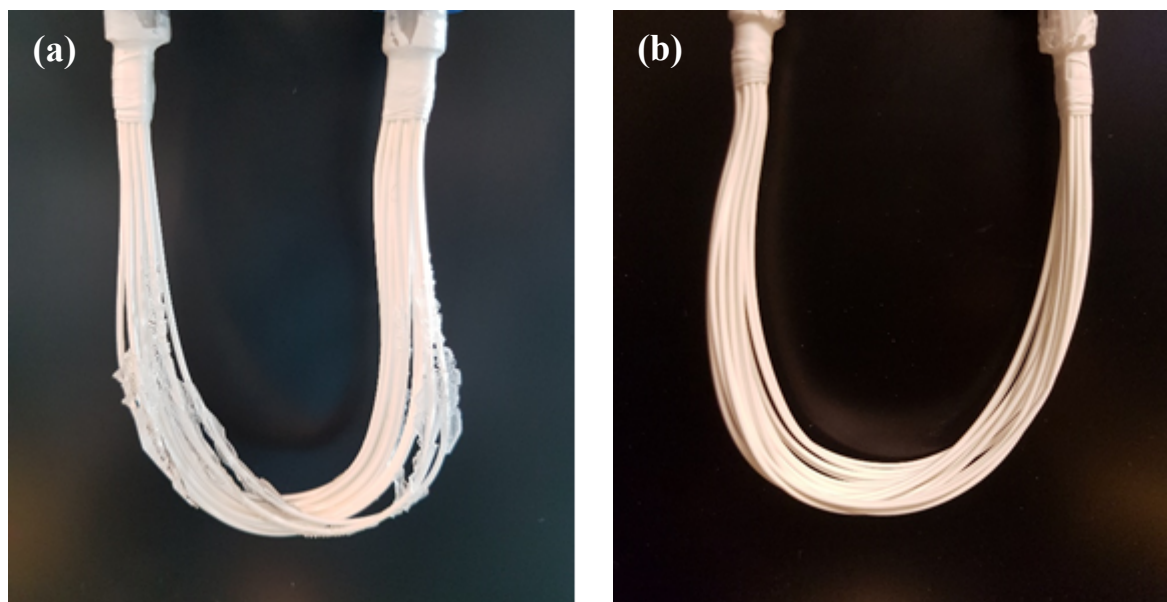
270 In S-DCMD configuration, generally, the membrane surface feed temperature is lower
271 compared to bulk feed temperature due to direct contact with cold permeate on the membrane
272 surface. This factor plays a prevalent role in the solubility of certain crystal salts that are especially
273 influenced by the effect of temperature. One such salt is Na_2SO_4 , which exhibits lower solubility at
274 low temperature (91 g/L @ 10 °C, and 195 g/L @ 20 °C) and higher solubility at increased
275 temperature (488 g/L @ 40 °C). This characteristic of Na_2SO_4 can lead to higher saturation state on
276 the membrane surface, and aggravate the formation of crystals. This results in the non-continuity of
277 MDC process.

278 The effect of this phenomenon can be mitigated in F-SMDC by creating and maintaining CG
279 in the reactor. The feed concentration (under 195 g/L) was lower at the top portion of the reactor
280 which contains the submerged membrane. Here, the direct contact with the permeate solution
281 (16.5 ± 0.2 °C) lowered the feed solution temperature which was set at 50.0 ± 1.3 °C. Specifically, the
282 feed concentration at the top portion of the reactor was maintained at 171.8 ± 5.1 g/L in cycle 1 and
283 169.2 ± 3.0 g/L in cycle 2. At these concentration ranges of Na_2SO_4 , super-saturation was not reached
284 at 16.5 ± 0.2 °C (feed temperature at bottom portion). As such, salt precipitation followed by crystal
285 deposition on the membrane surface was delayed up to around VCF 3.0 as shown in **Figure 8**. In
286 both cycles 1 and 2, fouling on the membrane surface was not detected due to the lower
287 concentration at the top portion. However, in cycle 1, the fouling phenomenon on the membrane
288 surface was detected after VCF 3.0 (**Figure 9**). This was due to rapid increase of concentration
289 (214.4 to 385.5 g/L) upon reaching VCF 3.0. Rapid flux decline occurred beyond this point (**Figure**
290 **8**).



291

292 **Figure 8** Flux and concentration variation in continuous F-SMDC (without crystal extraction until the
 293 completion of each cycle).



294 **Figure 9** Used membrane with Na_2SO_4 treatment at the end of (a) cycle 1, (b) cycle 2.

295

296 Initial crystal formation at the bottom portion of the reactor occurred at around VCF 2.2 in
 297 both cycles. At VCF 2.8 and above, the bottom portion of the reactor was completely filled with
 298 crystals. At this point, the feed concentration at the top portion of the reactor increased rapidly, and
 299 CG in the F-SMDC feed reactor was no longer maintained. As such, it is essential to continuously

300 extract crystals generated at the bottom portion of the reactor to maintain a feed concentration
301 gradient in the F-SMDC process. For this reason, an external crystallizer was used in this study as
302 described in section 2.1.

303 At the end of each operation cycle, Na₂SO₄ solution remained at the top and middle portions
304 of the reactor. It must be highlighted that the F-SMDC was carried out in a batch mode. In the
305 scenario of a continuous mode operation, periodic crystal extraction from the bottom portion of the
306 reactor would be possible. This would enable continuous crystal growth simultaneously, while
307 achieving near zero liquid discharge in the reactor. However, in view of the batch mode operation of
308 this study, an external crystallization was used to evaluate the potential of further crystal growth with
309 the remaining Na₂SO₄ solution. This would enable to depict the near zero liquid discharge scenario
310 of a continuous mode. In depth evaluation of F-SMDC operation in a continuous mode will be
311 explored in future studies to establish this scenario.

312 Upon allowing the reactor to stand at room temperature (23.2±0.3 °C) for 3 days (72 h),
313 further salt crystallization occurred due to its super-saturated state (**Table 2**). This step enabled the
314 generation of additional crystals, thereby, increasing the total amount of crystals. Although the initial
315 concentrations in both cycles were different (because of different degree of concentrate: VCF 3.5 in
316 cycle 1 vs. VCF 3.0 in cycle 2), the final concentrations of both cycles were similar. However, the
317 solution volume reduction ratio varied (87% in cycle 1 vs. 47% in cycle 2) (**Table 2**). The simple
318 step of allowing the feed solution to remain at room temperature without additional treatment
319 enabled to decrease the feed concentration and volume by 32% and 46% respectively. Further, the
320 small quantity of remaining solution at the top and middle portions of the reactor can be channelled
321 back to the bulk feed tank for a subsequent F-SMDC operation cycle. This indicated that F-SMDC
322 with external crystallization does have the potential to achieve near zero liquid discharge.

323 **Table 2** Volume and concentration of feed solution extracted from reactor upon F-SMDC and upon
 324 external crystallization (standing at room temperature for 24 - 72 h).

Sample	1 st cycle		2 nd cycle	
	Concentration (g/L)	Amount (mL)	Concentration (g/L)	Amount (mL)
Final F-SMDC feed (Before crystallization)	329.4±6.1	1140	218.1±2.3	1160
Upon external crystallization	160.4±0.2 (24 h)	150	160.4±0.7 (24 h)	620
	149.9±2.3 (72 h)		147±0.3 (72 h)	

325

326 4.3. Crystal production in F-SMDC

327 In F-SMDC, crystals were generated at the bottom portion of the reactor due to high
 328 concentration and lower temperature setting. In this study, the bottom portion of the reactor was
 329 cooled down up to 20.0±0.5 °C while the top portion of the reactor was maintained at 50.0±1.3 °C.
 330 At the bottom portion of the reactor, the combined condition of higher feed concentration and lower
 331 temperature enabled to achieve a faster super-saturation state of Na₂SO₄ compared to the top portion
 332 of the reactor. The CG and TG in the F-SMDC (lower concentration and higher temperature at top
 333 portion, higher concentration and lower temperature at bottom portion) improved the efficiency of
 334 recovering valuable crystals as well as obtaining higher water recovery and better stability (lower
 335 scaling) of MD process.

336 When 120 g/L Na₂SO₄ was treated without using crystals extraction, crystals were generated
 337 both at the top and bottom portions of the reactor. The amount of generated crystals formed was

338 directly proportional to the concentration ratio of feed solution (**Table 3**). High amount of crystals
 339 was generated both during cycle 1 (1169.0 g) and cycle 2 (898.0 g). In the case of cycle 1, F-SMDC
 340 operation was carried on beyond the point of rapid flux decline in order to obtain a highly
 341 concentrated final solution. The rapid permeate flux decline due to fouling and high feed
 342 concentration degraded the stability of the process. Therefore, it is not recommended to operate F-
 343 SMDC beyond the super-saturation state of the feed solution in the future study.

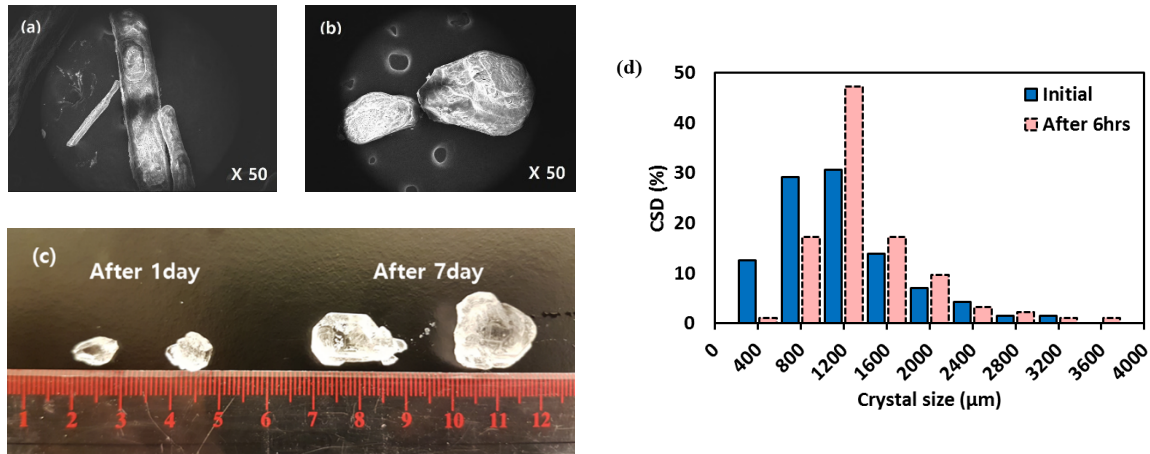
344 **Table 3** Crystal and fresh water production by F-SMDC operation (feed: Na₂SO₄).

Sources	1 st cycle		2 nd cycle	
	Produced crystal (g)	Produced fresh water (mL)	Produced crystal (g)	Produced fresh water (mL)
Bottom portion of the reactor	551.3		541.6	
External crystallizer (containing saturated solution from top and middle portion of the reactor)	617.7	4295.5 (99% ion rejection)	356.4	3561.4 (99% ion rejection)
Total	1169.0		898.0	

345

346 The crystal production rate can be increased by factors such as temperature control, crystal
 347 size and immersion of crystals into saturated solution. As shown in **Table 2**, the volume and
 348 concentration of mother liquid decreased due to the formation of Na₂SO₄ crystals with time. For
 349 instance, the feed concentration of 160.4±0.2 g/L after 24 h was reduced to 149.9±2.3 g/L after 72 h.
 350 This indicated that additional crystals of larger sizes can be produced by the immersion of initial
 351 crystals into the mother liquid (**Figure 10(d)**). The morphology of Na₂SO₄ crystals changed from

352 rectangle shape to spherical shape over time (**Figure 10(a), (b) and (c)**). Prevalent growth and
 353 change in shape of crystals were detected on crystals that were fully immersed in the mother liquid.
 354 The results indicated that direct contact with mother liquid would enhance the growth of crystals. It
 355 is therefore essential to have enough contact area and immersion time with mother liquid. By doing
 356 so, a narrow size distribution of the crystals can be obtained.



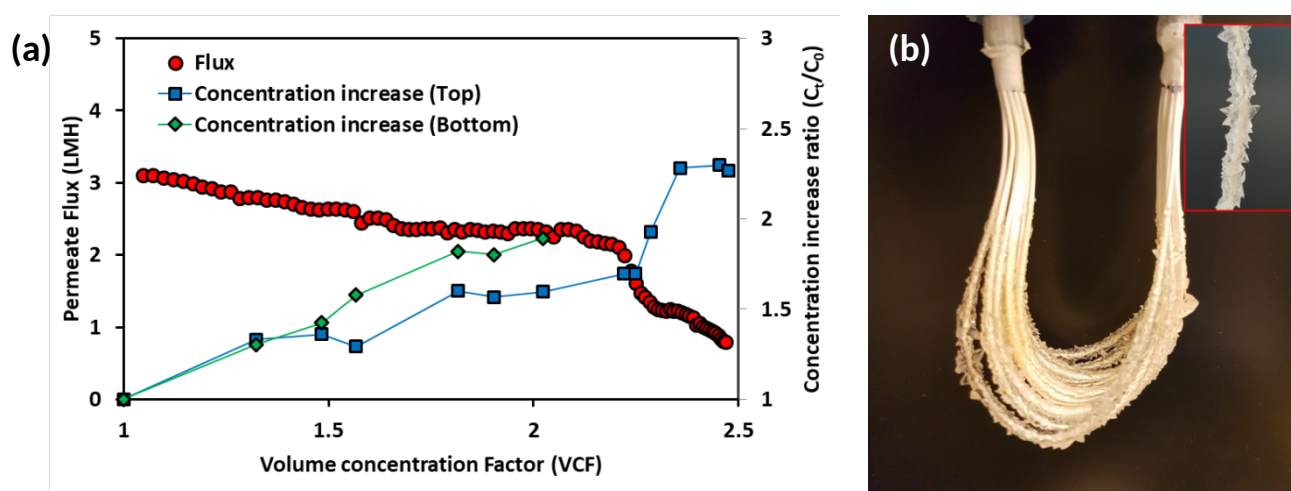
357 **Figure 10** Crystal size distribution (CSD) and change in morphology of produced Na_2SO_4 crystals with
 358 time. Images of crystals at (a) initial, and after (b) 60min and (c) 1 day and 7 days, and (d) size distribution of
 359 Na_2SO_4 .

360

361 4.4. Effect of salinity

362 The effect of salinity in the treatment of Na_2SO_4 solution was examined by adding NaCl . As
 363 shown in **Figure 11**, the concentration gradient trend at the initial stage (up to VCF 1.5) was similar
 364 with and without the presence of NaCl . In the presence of NaCl , the formation of crystals at the
 365 bottom portion of the reactor started from around VCF 1.8, while the concentration at the top portion
 366 of the reactor increased (with and without the presence of NaCl), lower VCF was achieved in the
 367 presence of NaCl . In the presence of NaCl , from VCF 2.2 onwards, visible presence of crystals was
 368 observed. At the same time, rapid flux decline and increase of feed concentration at the top portion

369 of the reactor occurred. This occurrence was associated to the presence of crystals on the membrane
 370 surface. The F-SMDC operation condition, namely concentrated feed solution and cooler membrane
 371 surface condition (direct contact with cold permeate) enabled the generation of CG. The crystal
 372 deposition on the membrane surface reduced the effective membrane area. This decreased the rate of
 373 concentration and degree of cooling by permeate, resulting in reduced crystallization of concentrated
 374 solution. Therefore, concentrated solution remained at the vicinity of the membrane boundary layer,
 375 and feed concentration at the top portion of the reactor portion increased by diffusion. This caused an
 376 increased crystal deposition onto the membrane surface (**Figure 11 (b)**).



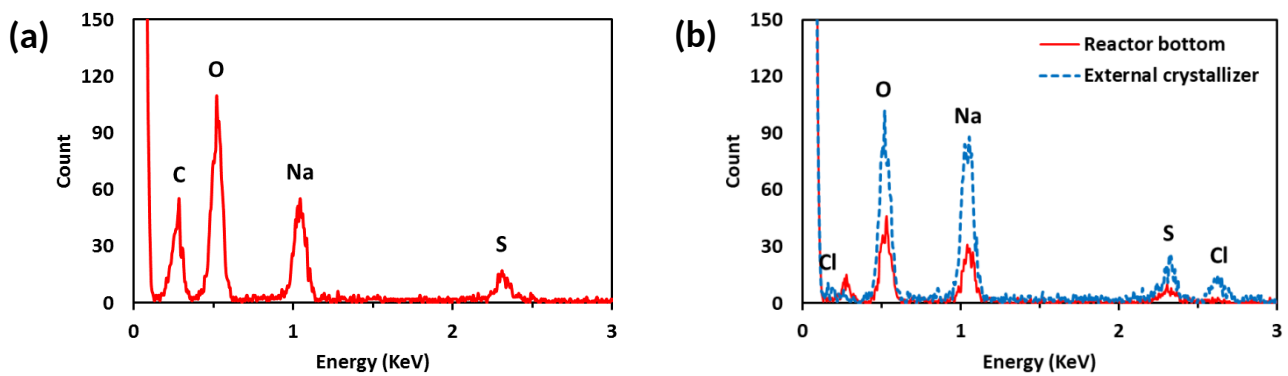
377 **Figure 11** F-SMDC with Na_2SO_4 and NaCl : (a) variation of flux and concentration at the top and bottom
 378 portion of the reactor, (b) used membrane at the end of the experiment.

379

380 The EDX analysis revealed the presence of sodium, oxygen and sulphur elements on the used
 381 membrane surface and at the bottom portion of the reactor (**Figure 12(a)** and **(b)**). On the other hand,
 382 chloride ion was detected in crystals generated in feed solution of the top and middle portions of the
 383 reactor. The results indicated that a separate generation of crystal from solution can be achieved by a
 384 control of concentration and temperature at suitable range. In addition, the concentration of sodium
 385 ion in solution seems to influence crystallization phenomenon on the membrane surface and at the

386 bottom portion of the reactor. The crystallization on the membrane surface was detected at around
387 VCF 3.3 in the absence of NaCl. The crystals formation on the membrane surface became faster
388 (around VCF 2.2) with NaCl. At this point, the concentrations of sodium ion in both feed solutions
389 with and without NaCl were similar (93.08 g/L without NaCl and 93.28 g/L with NaCl). Also, upon
390 crystal formation at the bottom portion of the reactor, similar amount of sodium ion concentration
391 was observed in both the feed solutions (without NaCl: 107.78 g/L in cycle 1 / 106.26 g/L in cycle 2,
392 and with NaCl: 106.08 g/L). The difference in the initial point of crystallization on the membrane
393 surface and at the bottom of the reactor was attributed to temperature difference.

394



395 **Figure 12** EDX analysis of crystals (a) deposited on the used membrane surface, (b) produced from the
396 bottom portion of the reactor and external crystallizer (saturated feed solution from the top and middle portion
397 of the reactor) (feed solution: Na₂SO₄ and NaCl).

398

399 5. Conclusions

400 The feasibility of fractional submerged membrane distillation-crystallization (F-SMDC)
401 process was evaluated using a feed solution containing high concentration of Na₂SO₄ without and
402 with NaCl. The following conclusions were made from the experimental investigation:

- 403 • F-SMDC setting enabled the creation of CG and TG using a partition and double wall
404 heating/cooling in the feed reactor. A lower feed concentration and higher feed temperature
405 was maintained at the top portion of the reactor. Meanwhile, higher feed concentration and
406 lower feed temperature was maintained at the bottom portion of the reactor.
- 407 • The presence of CG/TG in F-SMDC enabled to achieve higher water recovery (VCF 3.5) and
408 lower membrane scaling, compared to SMDC mode (VCF 2.9).
- 409 • The condition of elevated feed concentration and lower temperature at the bottom portion of
410 the reactor was favourable for high crystal formation in F-SMDC.
- 411 • The presence of salt (NaCl) influenced the crystallization of Na_2SO_4 at the bottom portion of
412 the reactor and on the membrane surface, resulting in higher crystallization in both locations.
- 413 • F-SMDC was effective in reducing membrane scaling, producing high quality fresh water
414 and valuable crystals (Na_2SO_4).
- 415 • The shape and dimension of F-SMDC reactor are essential factors that influence the
416 formation of CG/TG and the overall F-SMCD performance. Further optimization of the
417 reactor configuration is an important factor that must be explored in detail.

418

419 **Acknowledgement**

420 This work was funded by Australian Research Council Discovery Research Grant (DP150101377)
421 and two Basic Science Research Programs through the National Research Foundation of Korea
422 (NRF) funded by the Ministry of Education (2017R1A6A3A04004335) and the Ministry of Science,
423 ICT, & Future Planning (2017R1A2B3009675).

425 **References**

- 426 [1] L.A. Hoover, W.A. Phillip, A. Tiraferri, N.Y. Yip, M. Elimelech, Forward with osmosis: Emerging
427 applications for greater sustainability, *Environmental Science and Technology*, 45 (2011) 9824-9830.
- 428 [2] J. Cebrian, C.M. Duarte, Detrital stocks and dynamics of the seagrass *Posidonia oceanica* (L.) Delile in the
429 Spanish Mediterranean, *Aquatic Botany*, 70 (2001) 295-309.
- 430 [3] Y. Choi, G. Naidu, S. Jeong, S. Vigneswaran, S. Lee, R. Wang, A.G. Fane, Experimental comparison of
431 submerged membrane distillation configurations for concentrated brine treatment, *Desalination*, 420 (2017)
432 54-62.
- 433 [4] X. Ji, E. Curcio, S. Al Obaidani, G. Di Profio, E. Fontananova, E. Drioli, Membrane distillation-
434 crystallization of seawater reverse osmosis brines, *Separation and Purification Technology*, 71 (2010) 76-82.
- 435 [5] G. Naidu, S. Jeong, Y. Choi, S. Vigneswaran, Membrane distillation for wastewater reverse osmosis
436 concentrate treatment with water reuse potential, *Journal of Membrane Science*, 524 (2017) 565-575.
- 437 [6] Y. Choi, G. Naidu, S. Jeong, S. Lee, S. Vigneswaran, Effect of chemical and physical factors on the
438 crystallization of calcium sulfate in seawater reverse osmosis brine, *Desalination*, 426 (2018) 78-87.
- 439 [7] G. Naidu, S. Jeong, Y. Choi, M.H. Song, U. Oyunchuluun, S. Vigneswaran, Valuable rubidium extraction
440 from potassium reduced seawater brine, *Journal of Cleaner Production*, 174 (2018) 1079-1088.
- 441 [8] S. Jeong, G. Naidu, R. Vollprecht, T. Leiknes, S. Vigneswaran, In-depth analyses of organic matters in a
442 full-scale seawater desalination plant and an autopsy of reverse osmosis membrane, *Separation and*
443 *Purification Technology*, 162 (2016) 171-179.
- 444 [9] D. Squire, Reverse osmosis concentrate disposal in the UK, *Desalination*, 132 (2000) 47-54.
- 445 [10] D. Squire, J. Murrer, P. Holden, C. Fitzpatrick, Disposal of reverse osmosis membrane concentrate,
446 *Desalination*, 108 (1997) 143-147.

- 447 [11] J.S. Ho, Z. Ma, J. Qin, S.H. Sim, C.-S. Toh, Inline coagulation–ultrafiltration as the pretreatment for
448 reverse osmosis brine treatment and recovery, *Desalination*, 365 (2015) 242-249.
- 449 [12] P. Loganathan, G. Naidu, S. Vigneswaran, Mining valuable minerals from seawater: a critical review,
450 *Environmental Science: Water Research & Technology*, 3 (2017) 37-53.
- 451 [13] G. Naidu, S. Jeong, M.A.H. Johir, A.G. Fane, J. Kandasamy, S. Vigneswaran, Rubidium extraction from
452 seawater brine by an integrated membrane distillation-selective sorption system, *Water Research*, 123 (2017)
453 321-331.
- 454 [14] H. Julian, S. Meng, H. Li, Y. Ye, V. Chen, Effect of operation parameters on the mass transfer and
455 fouling in submerged vacuum membrane distillation crystallization (VMDC) for inland brine water treatment,
456 *Journal of Membrane Science*, 520 (2016) 679-692.
- 457 [15] F. Edwie, T.-S. Chung, Development of simultaneous membrane distillation–crystallization (SMDC)
458 technology for treatment of saturated brine, *Chemical Engineering Science*, 98 (2013) 160-172.
- 459 [16] S. Meng, Y. Ye, J. Mansouri, V. Chen, Crystallization behavior of salts during membrane distillation
460 with hydrophobic and superhydrophobic capillary membranes, *Journal of Membrane Science*, 473 (2015)
461 165-176.
- 462 [17] C.M. Tun, A.G. Fane, J.T. Matheickal, R. Sheikholeslami, Membrane distillation crystallization of
463 concentrated salts—flux and crystal formation, *Journal of Membrane Science*, 257 (2005) 144-155.
- 464 [18] F. Macedonio, E. Drioli, Hydrophobic membranes for salts recovery from desalination plants,
465 *Desalination and Water Treatment*, 18 (2010) 224-234.
- 466 [19] C.A. Quist-Jensen, F. Macedonio, D. Horbez, E. Drioli, Reclamation of sodium sulfate from industrial
467 wastewater by using membrane distillation and membrane crystallization, *Desalination*, 401 (2017) 112-119.

- 468 [20] G. Naidu, W.G. Shim, S. Jeong, Y. Choi, N. Ghaffour, S. Vigneswaran, Transport phenomena and
469 fouling in vacuum enhanced direct contact membrane distillation: Experimental and modelling, *Separation*
470 *and Purification Technology*, 172 (2017) 285-295.
- 471 [21] A. Alkudhiri, N. Darwish, N. Hilal, Membrane distillation: A comprehensive review, *Desalination*, 287
472 (2012) 2-18.
- 473 [22] A. Ali, F. Macedonio, E. Drioli, S. Aljlil, O.A. Alharbi, Experimental and theoretical evaluation of
474 temperature polarization phenomenon in direct contact membrane distillation, *Chemical Engineering Research*
475 *and Design*, 91 (2013) 1966-1977.
- 476 [23] H. Lu, J. Wang, T. Wang, N. Wang, Y. Bao, H. Hao, Crystallization techniques in wastewater treatment:
477 An overview of applications, *Chemosphere*, 173 (2017) 474-484.
- 478 [24] S. Meng, Y.-C. Hsu, Y. Ye, V. Chen, Submerged membrane distillation for inland desalination
479 applications, *Desalination*, 361 (2015) 72-80.
- 480 [25] L. Francis, N. Ghaffour, A.S. Al-Saadi, G.L. Amy, Submerged membrane distillation for seawater
481 desalination, *Desalination and Water Treatment*, 55 (2015) 2741-2746.
- 482 [26] F. Edwie, T.-S. Chung, Development of hollow fiber membranes for water and salt recovery from highly
483 concentrated brine via direct contact membrane distillation and crystallization, *Journal of Membrane Science*,
484 421-422 (2012) 111-123.
- 485 [27] Y. Shin, J. Sohn, Mechanisms for scale formation in simultaneous membrane distillation crystallization:
486 Effect of flow rate, *Journal of Industrial and Engineering Chemistry*, 35 (2016) 318-324.
- 487 [28] L.D. Tijing, Y.C. Woo, J.-S. Choi, S. Lee, S.-H. Kim, H.K. Shon, Fouling and its control in membrane
488 distillation—A review, *Journal of Membrane Science*, 475 (2015) 215-244.
- 489 [29] S. Goh, J. Zhang, Y. Liu, A.G. Fane, Fouling and wetting in membrane distillation (MD) and MD-
490 bioreactor (MDBR) for wastewater reclamation, *Desalination*, 323 (2013) 39-47.

491 [30] Y. Choi, S. Vigneswaran, S. Lee, Evaluation of fouling potential and power density in pressure retarded
492 osmosis (PRO) by fouling index, *Desalination*, 389 (2016) 215-223.

Highlights

- Fractional-submerged MDC (F-SMDC) showed promising potential for brine treatment.
- Concentration/temperature gradients (CG/TG) in F-SMDC reactor was beneficial.
- High TG/low CG at reactor top enabled to reduce the scaling on MD membrane.
- Low TG/high CG at reactor bottom was favourable for sodium sulphate crystallization.
- Stable CG/TG in F-SMDC required periodic crystal extraction from the reactor.

Fractional-submerged membrane distillation crystallizer (F-SMDC) for treatment of high salinity solution

Youngkwon Choi^a, Gayathri Naidu^a, Sanghyun Jeong^b, Sangho Lee^c, Saravanamuthu Vigneswaran^{a,*}

^a Faculty of Engineering, University of Technology Sydney (UTS), P.O Box 123, Broadway, NSW 2007 Australia,

^b Graduate School of Water Resources, Sungkyunkwan University (SKKU), 2066, Seobu-ro, Jangan-gu, Suwon-si, Gyeonggi-do, 16419, Republic of Korea,

^c School of Civil and Environmental Engineering, Kookmin University, Seoul 136-702, Republic of Korea

*Corresponding author: Tel +61-2-9514-2641; Fax +61-2-9514-2633; Email: Saravanamuthu.Vigneswaran@uts.edu.au

Abstract

Membrane distillation with crystallization (MDC) is an attractive process for high saline seawater reverse osmosis (SWRO) brine treatment. MDC produces additional fresh water while simultaneously recovering valuable resources. This study developed a novel approach of fractional-submerged MDC (F-SMDC) process, in which MD and crystallizer are integrated in a feed tank with a submerged membrane. F-SMDC principle is based on the presence of temperature/concentration gradient (TG/CG) in the feed reactor. The operational conditions at the top portion of the feed reactor (higher temperature and lower feed concentration) was well suited for MD operation, while the bottom portion of the reactor (lower temperature and higher concentration) was favourable for crystal growth. F-SMDC performance with direct contact MD to treat brine and produce sodium sulfate (Na_2SO_4) crystals using TG/CG showed positive results. The TG/CG approach in F-SMDC enabled to achieve higher water recovery for brine treatment with a volume concentration factor

23 (VCF) of over 3.5 compared to VCF of 2.9 with a conventional S-MDC set-up. Further, the high
24 feed concentration and low temperature at the reactor bottom in F-SMDC enabled the formation of
25 Na_2SO_4 crystals with narrow crystal size distribution.

26 **Keywords:** Concentration and temperature gradients; Membrane distillation with fractional
27 crystallization; Resource recovery; Seawater reverse osmosis brine; Sodium sulfate crystal

29 **1. Introduction**

30 Reverse osmosis (RO) based seawater desalination (i.e. SWRO) technology has been widely
31 used to solve global water crisis of fresh water shortage owing to its affordable operation cost and
32 reliability [1-3]. However, one of the major limitations of SWRO is its low recovery (30~50%),
33 resulting in the production of a substantially large amount of concentrated brine that has to be
34 managed [4-6]. The SWRO brine management incurs an additional operating cost to the plant as
35 well as environmental issues when SWRO brine is discharged directly into the environment [7].
36 SWRO brine contains a variety of chemicals (coagulant, chemical washing agent, and pH adjusting
37 agent) which are employed during SWRO process, Also, SWRO brine contains a high concentration
38 of organic and inorganic matters [8-11]. In recent times, simultaneous brine treatment with
39 extraction/production of valuable resources is favoured to offset the treatment cost rather than the
40 approach of treatment followed by disposal. The former is also preferred as give than seawater and
41 likewise seawater brine contains a number valuable elements [12, 13].

42 In this regard, membrane distillation with crystallizer (MDC) shows promising potential in
43 SWRO brine treatment [14-18]. MDC is an integrated process that can achieve high quality fresh
44 water while simultaneously extracting valuable resources from high salinity solution [14]. MDC is
45 attractive compared to traditional crystallization processes because of the following factors: well-
46 controlled saturation rate, faster nucleation rate and reduction of induction time [19]. Moreover, the
47 ability to concentrate solution up to a saturation point with minimal flux decline is an added
48 advantage of MDC [20-22]. Cooling crystallization method is widely used in separation processes
49 for solution having different solubility at different temperatures due to its ease of control and
50 maintenance [23]. However, one of the major limitations is the significant energy consumption due
51 to initial heating (thermal MD operation) followed by cooling for the crystallization.

52 A number of methods such as submerged MD (SMD) have been evaluated in terms of energy
53 consumption and economic benefits to improve the efficiency of conventional MDC process [3, 24,
54 25]. For instance, in SMD process, channelling heated feed solution through a pump to the
55 membrane module can be eliminated, which results in lower heat losses through the feed channel
56 [14, 26]. In this case, the feed tank can also act as a crystallizer, achieving an integrated system [3].
57 Nevertheless, several limitations are still present such as challenging saturated feed concentration
58 effect, and fouling caused by crystal formation in the feed tank as well as on the membrane [27-29].
59 Previous studies have shown that at elevated feed concentration levels [3], MD performance is
60 affected by flux decline and wetting phenomenon. This decreases the membrane life span, resulting
61 in more frequent membrane replacement, incurring addition operation cost [30].

62 In view of this, fractional submerged MDC (F-SMDC) based on principle of maintaining a
63 feed concentration gradient (CG) and feed temperature gradient (TG) in the reactor was evaluated in
64 this study. Maintaining CG and TG in the feed reactor can positively influence both MD and
65 crystallization. CG and TG in the reactor enables to reduce feed concentration and increase feed
66 temperature at the top portion of the reactor where the submerged membrane is located.
67 Simultaneously, the bottom portion of the reactor maintains high feed concentration with low feed
68 temperature which enhances crystallization at the bottom portion of the reactor. This is due to the
69 formation of high saturation state at the bottom portion of the reactor where crystals form
70 continuously during F-SMDC operation. This setting potentially promises higher water recovery,
71 with reduced membrane scaling issues. Further, the continuous extraction of crystal from the bottom
72 of the reactor is expected to reduce the salt contents in feed solution [14].

73 In this study, the feasibility of F-SMDC for the treatment of highly concentrated and saline
74 feed solution was investigated and compared with conventional submerged membrane distillation
75 crystallization (SMDC). The trend of CG/TG in the feed reactor was examined during the operation.

76 The effect on the flux and crystallization efficiency in the F-SMDC was evaluated. In addition,
77 methods to improve the efficiency of maintaining CG/TG in the feed reactor were investigated.

78

79 **2. Materials and Methods**

80 **2.1 Lab-scale setup**

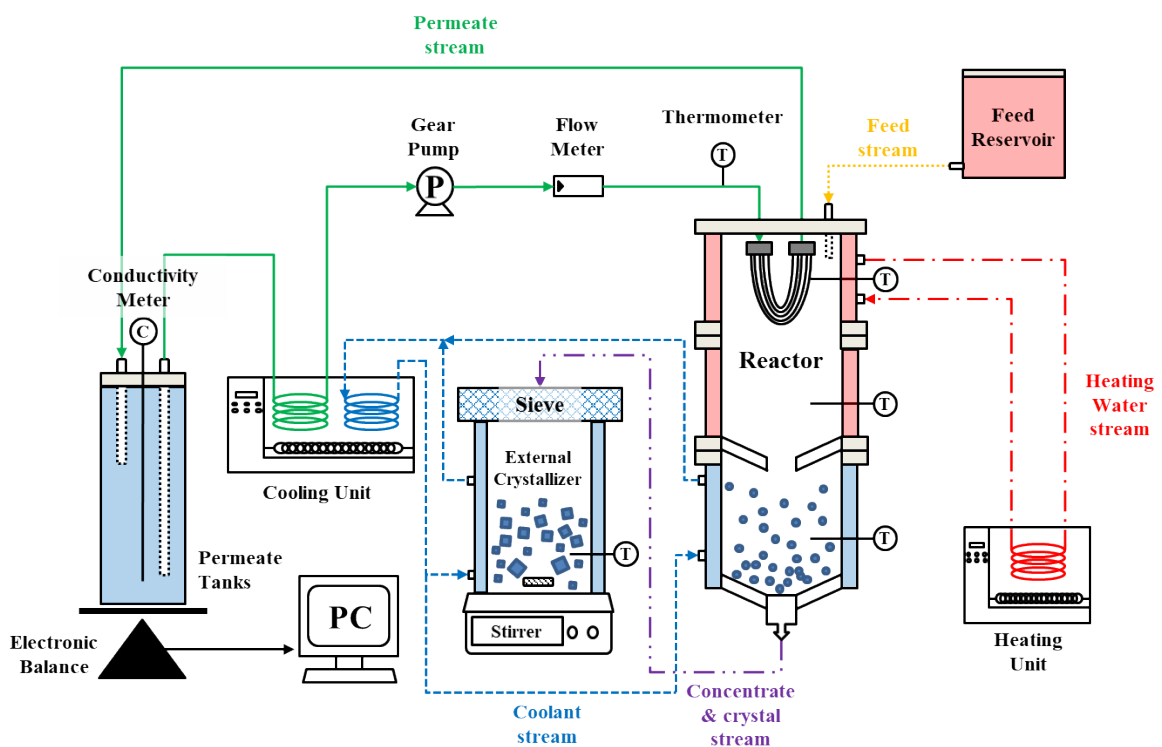
81 F-SMDC process with direct contact MD (DCMD) configuration based on GC and TG was
82 used in this study (**Figure 1**). The F-SMDC reactor consisted of three cylindrical cells with a height
83 of 150 mm and an inner diameter of 70 mm (volume of the single cell = 580 mL, and total volume of
84 the reactor = 1,740 mL). The reactor is equipped with double wall to enable the control of TG as
85 temperature control of feed solution is essential in the reactor (**Figure 2**). The partition in the shape
86 of funnel (length = 25 mm, and hole diameter = 20 mm) was installed between the top and bottom
87 portion. This partition acts as a barrier that minimized the mixing of solution by natural convection
88 caused by heating or cooling. Feed solution was placed inside of the reactor while heating and
89 cooling water was circulated at the outer wall of the reactor with respective heating and cooling
90 units. This enabled the feed solution at the top portion of the reactor to be maintained at 50.0 ± 1.3 °C,
91 while, the feed solution at the bottom portion of the reactor was maintained at 20.0 ± 1.5 °C.
92 Thermometer was placed in each cell to measure the temperature of feed solution in real-time.

93 Meanwhile, the permeate temperature (T_p) was maintained at 16.5 ± 0.2 °C, and was measured
94 using temperature sensors placed at the permeate channel. The permeate flow rate of 0.5 L/min was
95 controlled using a gear-pump. Feed solution was fed continuously into the top portion of the reactor
96 by the differential head of water between the reactor and feed tank. Continuous flow of new feed
97 solution to the top portion of reactor enables to maintain a constant feed solution concentration rather
98 than an increasing feed concentration. This systematically minimizes the effect of increased feed

99 concentration on MD performance. The temperature of feed solution in the feed tank (reservoir) was
100 maintained at room temperature (23.2 ± 0.3 °C).

101 An external crystallizer was used in the last stage of the F-SMDC operation. Upon attaining
102 super-saturation state at the bottom portion of the reactor, the remaining feed solution (mother liquid)
103 was fed to this external reactor. The external reactor was kept at room temperature (23.2 ± 0.3 °C)
104 with constant stirring (50 rpm) of the mother liquid to enhance crystal growth.

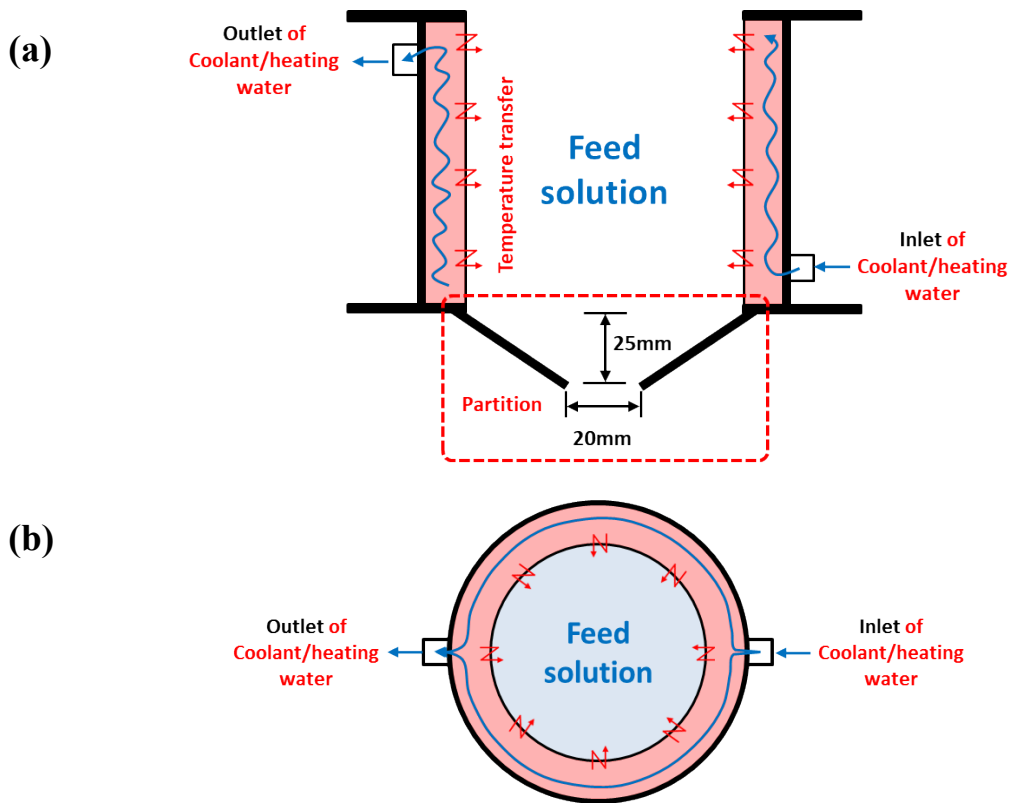
105 The permeate flux was calculated from on the solution mass difference with time using an
106 electronic balance. The permeate/fresh water quality was evaluated by measuring the
107 conductivity/total dissolved solids (TDS) value in real-time. All the experiments were duplicated to
108 ensure the reproducibility.



109
110 **Figure 1** Set-up of F-SMDC process: permeate stream (—), stream of continuous feeding to the
111 reactor (feed solution) (·····), stream of concentrate and crystal generated from the reactor to the crystal

112 growth cell (---), the stream of heating water for the top portion of the reactor (---), stream of coolant water
113 for the bottom portion of the reactor and the crystal growth cell (—).

114



115 **Figure 2** Details of F-SMDC reactor showing the double wall feature for generating FT gradient
116 (heating in the top portion of the reactor and cooling at the bottom portion of the reactor): (a) Cross-sectional
117 view, and (b) Aerial view.

118

119 2.2 Feed solution

120 The performance of F-SMDC process was investigated using 120 g/L Na_2SO_4 solution as
121 feed solution. The solubility of Na_2SO_4 in water varies significantly at different temperature (91 g/L
122 @ 10 °C, 195 g/L @ 20 °C, and 488 g/L @ 40 °C). A mixed solution containing sodium chloride

123 (NaCl) and Na₂SO₄ was then used to examine an effect of salinity on treatment of high concentration
124 Na₂SO₄ solution (

125 **Table 1**). Both feed solutions were prepared using reagent grade salts (Sigma-Aldrich).

126

127 **Table 1** Composition of model solution.

Ions	Concentration (mg/L)
Sodium (Na ⁺)	58,320
Sulfate (SO ₄ ²⁻)	81,150
Chloride (Cl ⁻)	30,020

128

129 **2.3 Membrane**

130 A hollow-fiber polyvinylidene fluoride (PVDF) membrane (Econity, Republic of Korea)
131 module was used. The membrane has a nominal pore size of 0.1 μm with an outer and inner diameter
132 of 1.2 mm and 0.7 mm (membrane wall thickness: 250mm), liquid entry pressure (LEP) of 2.0-2.3
133 bar, and contact angle of 106±2° (based on the specifications provided by the manufacturer). A
134 membrane module with an effective membrane area of 0.0136 m² was used. The membrane module
135 consisted of 18 fibers, each of 0.2 m in length, which were potted on both ends of membrane fiber.

136

137 **2.4 Analysis**

138 Crystal morphology was characterized by a field emission scanning electron microscopy
139 (FESEM, Zeiss supra 55VP, Carl Zeiss AG). The TDS and conductivity of the permeate were
140 measured with a portable water quality meter (HQ40d multi, Hach). The concentrated feed solution
141 was measured using calibrated conductivity curves made using different concentration of Na₂SO₄

142 (15, 30, 60, 180 and 300 g/L Na₂SO₄). The concentrated solution was vacuum filtered using a glass
143 microfiber filter (Whatman, Grade GF/C, pore = 1.2 μm) enabling the crystals in the solution to be
144 retained on the filter. The crystals were dried at room temperature (23.2±0.3 °C) for 120 h and the
145 dry weight of crystals was measured using an electronic balance. The crystal form and sizes were
146 evaluated using a microscopy method. In this method, at least 72 crystals were selected randomly,
147 and each crystal was measured using microscope with an image analyser (ImagePro7). The crystal
148 sizes were then quantified with a crystal size distribution (CSD) procedure.

149 Volume concentration factor (VCF) used in this study was based on the reactor volume and
150 the amount of produced fresh water. The total volume of feed solution in F-SMDC reactor was
151 maintained at a fixed volume (1,740 mL) with continuous feeding of feed solution at the same rate of
152 produced fresh water. If the rejection ratio of produced fresh water is 100% over time, the feed
153 solution concentration in the reactor would increase while the total volume of feed solution was
154 maintained. In this context, the VCF value was calculated as:

$$\text{VCF} = \frac{V_{\text{reactor}} + V_{\text{total, permeate}}}{V_{\text{reactor}}}$$

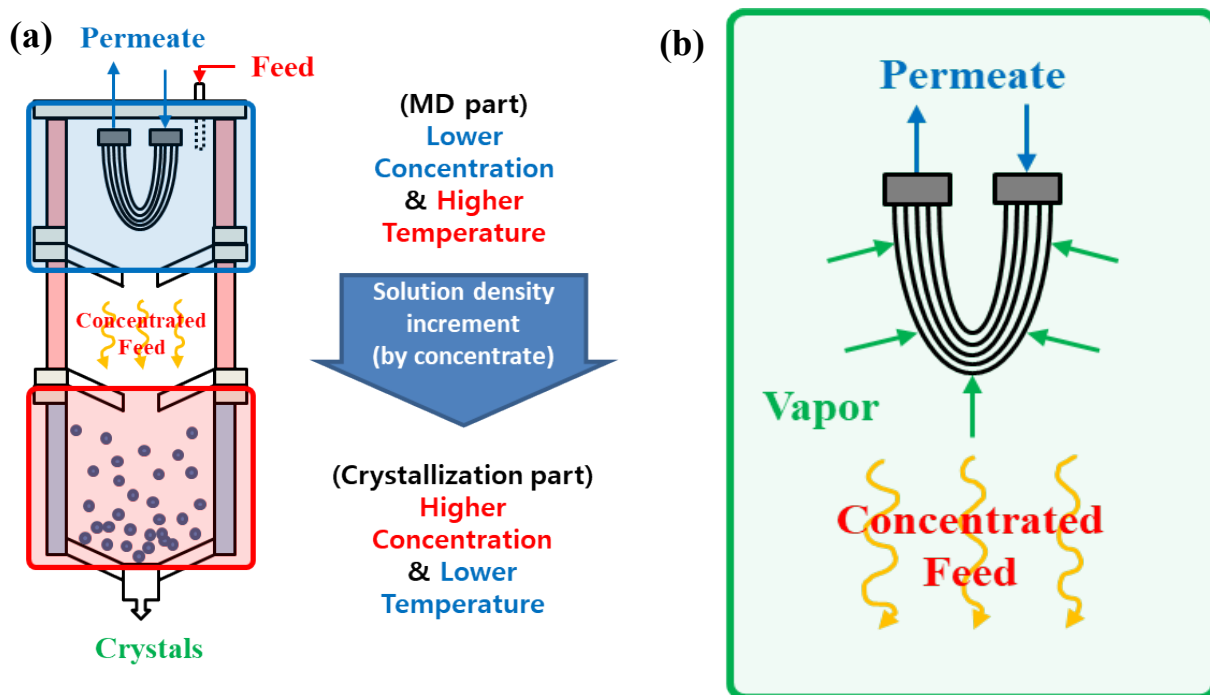
155

156 where V_{reactor} is the reactor volume, and $V_{\text{total,permeate}}$ is the total amount of permeate produced.

157 **3. F-SMDC principle**

158 F-SMDC is a combination of two processes: MD and crystallization in a single feed reactor
159 with a submerged membrane (**Figure 3(a)**). The submerged membrane module is placed at the top
160 portion of the feed reactor. In F-SMDC, a CG is generated in the feed reactor as a result of difference
161 in solution density. Upon the increase of feed solution concentration (MD part), the density of the
162 feed solution increases, resulting in the gravitation of concentrated feed solution to the bottom of the
163 reactor (**Figure 3(b)**). In S-DCMD, cooling down of feed solution by the cold permeate stream

164 further enhances this factor as water density is higher at low temperature. Accordingly, CG is
 165 generated in the reactor. Simultaneously, TG is generated by external heating and cooling of the
 166 outer wall (Figure 2).



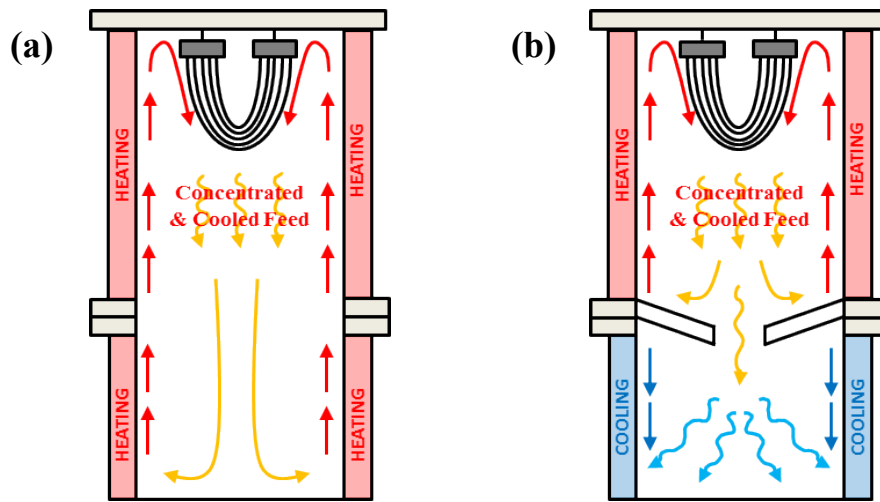
167 **Figure 3** Generation of concentration gradient (CG) in feed reactor of F-SMDC: (a) lower feed
 168 concentration at the top portion and higher feed concentration at the bottom portion, and (b) concentration
 169 effect at the top portion of the reactor containing submerged membrane.

170

171 The presence of CG in the feed reactor influences both MD and crystallization efficiency of
 172 the F-SMDC process. In MD, dissolved ion concentration in the feed solution is increased as the feed
 173 solution is concentrated, resulting in decrease of permeate flux. However, in crystallization process,
 174 elevated dissolved ion contents are favourable for attaining saturation degree of targeted compounds.
 175 Lower concentration at the top portion of the reactor is suitable for MD operation. Higher
 176 concentration at the bottom portion of the reactor is favourable for the formation of crystals since
 177 super-saturation (above the limits of metastable zone) of target salt should be reached to get a

178 nucleation of crystals. F-SMDC achieves an increase of feed concentration at the bottom portion of
179 the reactor at a faster ratio compared with theoretical concentration ratio in the whole reactor, and
180 crystals are formed when solution concentration exceeds the limits of metastable zone of solution.
181 Moreover, TG is formed in the reactor by the temperature transfer caused by movement of
182 concentrated feed solution to the bottom portion without additional temperature control (using
183 heating or cooling). Temperature at the top portion is higher than the bottom portion. The
184 maintenance of TG in F-SMDC enhances the crystallization phenomenon.

185 Convection current in the reactor occurs differently (**Figure 4(a)**). If feed solution is heated
186 up near the reactor wall, its density decreases with its expansion. As a result, it moves towards the
187 upper portion, and the unheated feed solution moves downwards. Moreover, concentrated and cooled
188 (because of the effect of lower permeate temperature (around 16.5 ± 0.2 °C) of S-DCMD) feed
189 solution by membrane operation favours the above effect. As a result, feed solution is mixed, and
190 therefore CG cannot be maintained in the feed reactor. Even though convection current effect on
191 solution mixing does not significantly affect CG, it should still be controlled to ensure that CG is
192 well controlled/maintained throughout the operation. In our design of F-SMDC, the incorporation of
193 a partition in the feed reactor enables to maintain convection current effect within the respective cells
194 (top and bottom portion of the reactor) (**Figure 4(b)**). The partition prevented the feed solution
195 mixing by convection current, resulting in maintaining CG and TG in the reactor.



196 **Figure 4** Convection current in reactor by heating and cooling of (a) conventional MDC process
 197 (reactor without cooling and partition) and (b) F-SMDC process (reactor with cooling and partition).

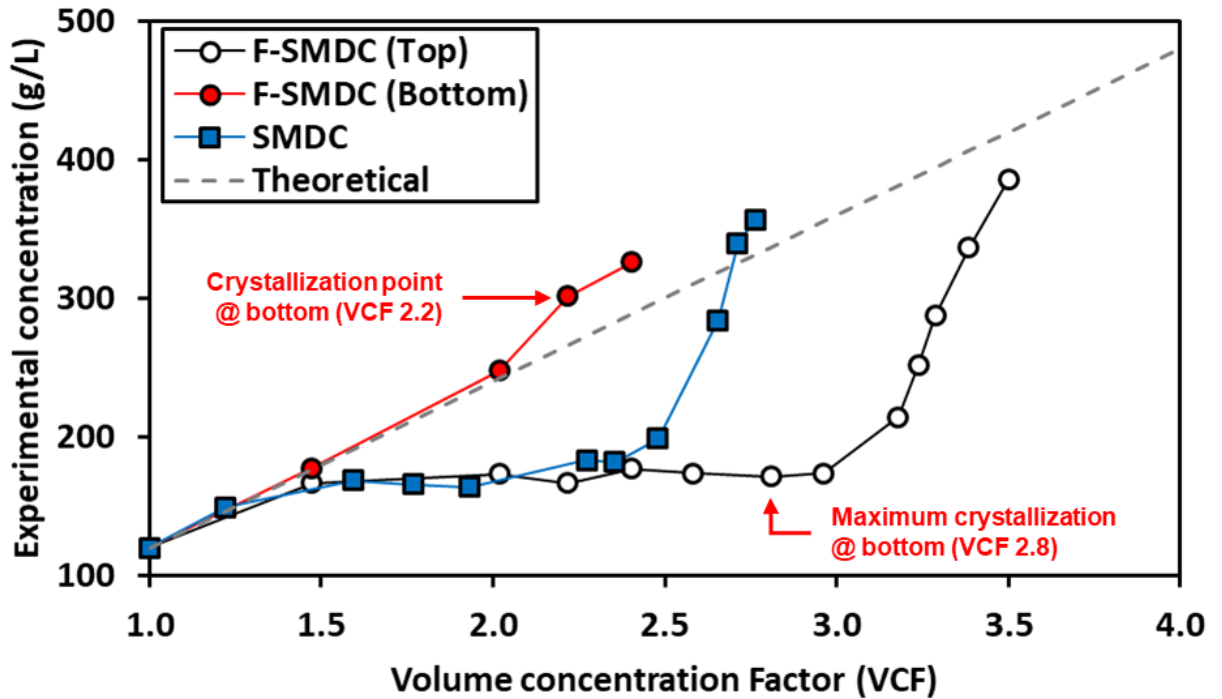
199 **4. Results and discussions**

200 In this study, the feasibility of F-SMDC was examined for the treatment of feed solution
201 containing Na₂SO₄ alone and with NaCl.

202 **4.1. Performance comparison of F-SMDC and SMDC**

203 The performance of conventional submerged MDC (SMDC) (reactor without cooling and
204 partitioning) was compared with F-SMDC (reactor with cooling and partitioning) under the same
205 operating conditions (reactor, feed temperature and feed solution) and same sampling points at the
206 top and bottom portion of the reactor. The initial flux of both SMDC and F-SMDC mode was 2.8 and
207 2.7 LMH respectively. The initial flux of S-MDC was slightly higher than F-SMDC, while the feed
208 solution concentration trend varied. Up to a feed solution VCF 2.5, a similar concentration variation
209 was observed for both SMDC and F-SMDC mode. However, in SMDC, above VCF 2.5, a rapid
210 increase of concentration from VCF 2.5 to 2.8 accompanied by a rapid flux decline was observed
211 (**Figures 5 and 6**). Both processes maintained 99% ion rejection ratio until the end of the experiment.
212 Comparatively, F-SMDC was able to maintain a stable concentrate (without rapid increase) up to
213 VCF 3.0 and sustained the operation up to VCF 3.5. The results indicated that in F-SMDC, the
214 partition between the top and the bottom portion of the reactor prevented the mixing of feed solution
215 by natural convection current, emulating a trap. This enabled to create a CG in the reactor, with a
216 higher concentration at the bottom portion of the reactor. In F-SMDC, the presence of CG in the feed
217 reactor was beneficial for both the MD and crystallization processes. Maintaining a low feed
218 concentration closer to the membrane in F-SMDC enabled to achieve a higher VCF (around VCF
219 3.5) with smaller flux decline compared to the SMDC (around VCF 2.8). In SMDC, concentrated
220 feed solution interferes with the transportation of vapour through the hydrophobic membrane,
221 decreasing its performance (reduced flux decline).

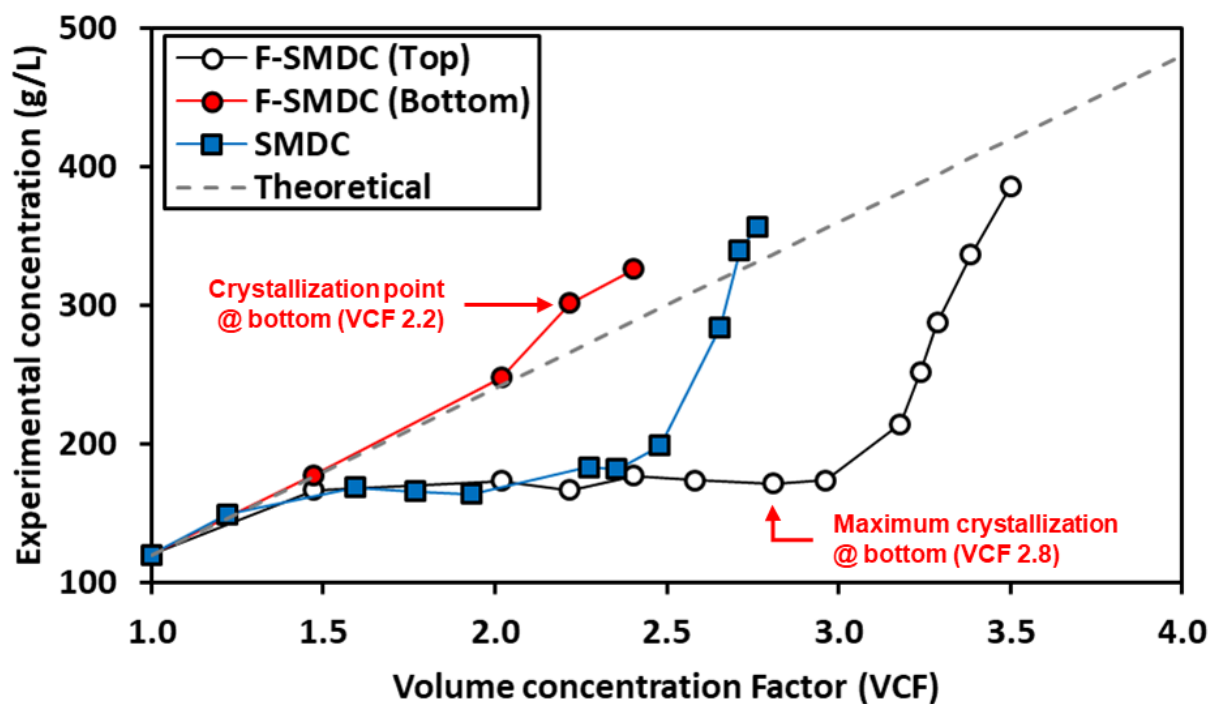
222 In F-SMDC, the presence of CG in the feed reactor was well reflected by the CG variation
223 between the top and bottom portion of the reactor (



224

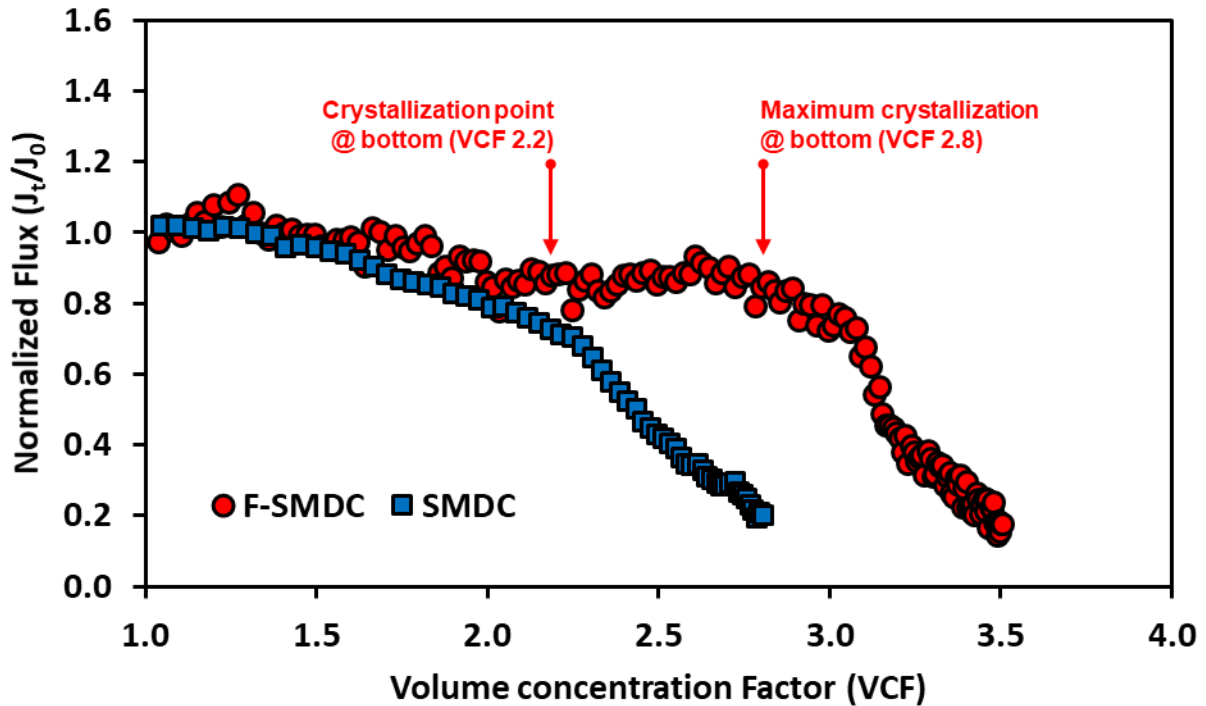
225 **Figure 5).** The CG effect was especially apparent from VCF 1.5 onwards. The feed
226 concentration at the top portion (MD part) of the reactor did not change rapidly while a rapid
227 increase of feed concentration at the bottom portion of the reactor was observed. At the top portion,
228 the feed solution concentration was maintained (range: 171.8 ± 5.1 g/L, 1.4 times of initial feed
229 concentration) below the theoretical feed concentration increment (initial feed concentration \times VCF).
230 Above VCF 2.0, feed concentration at the bottom portion of the reactor showed higher increment
231 than the theoretical feed concentration level. Over time, the feed concentration at the bottom portion
232 of the reactor greatly varied to the theoretical feed concentration. The results reflected the capacity of
233 F-SMDC to maintain a stable CG in the feed reactor.

234 In the F-SMDC mode, higher feed concentration at the bottom portion of the reactor than the
 235 top portion made it suitable for the formation of target crystals. Also, lower temperature (around 20.0
 236 ± 1.5 °C) at the bottom portion of the reactor, which was generated by the cooling as well as the
 237 movement of concentrated/cooled feed solution from the top portion (heated up) was favourable for
 238 the stimulation of crystals.



239

240 **Figure 5** Variation of feed concentration in the reactor during the operation in F-SMDC and SMDC
 241 modes (feed: Na₂SO₄).



242

243

Figure 6 Comparison of flux in F-SMDC and SMDC mode (without crystal extraction).

244

245

246

247

248

249

250

251

252

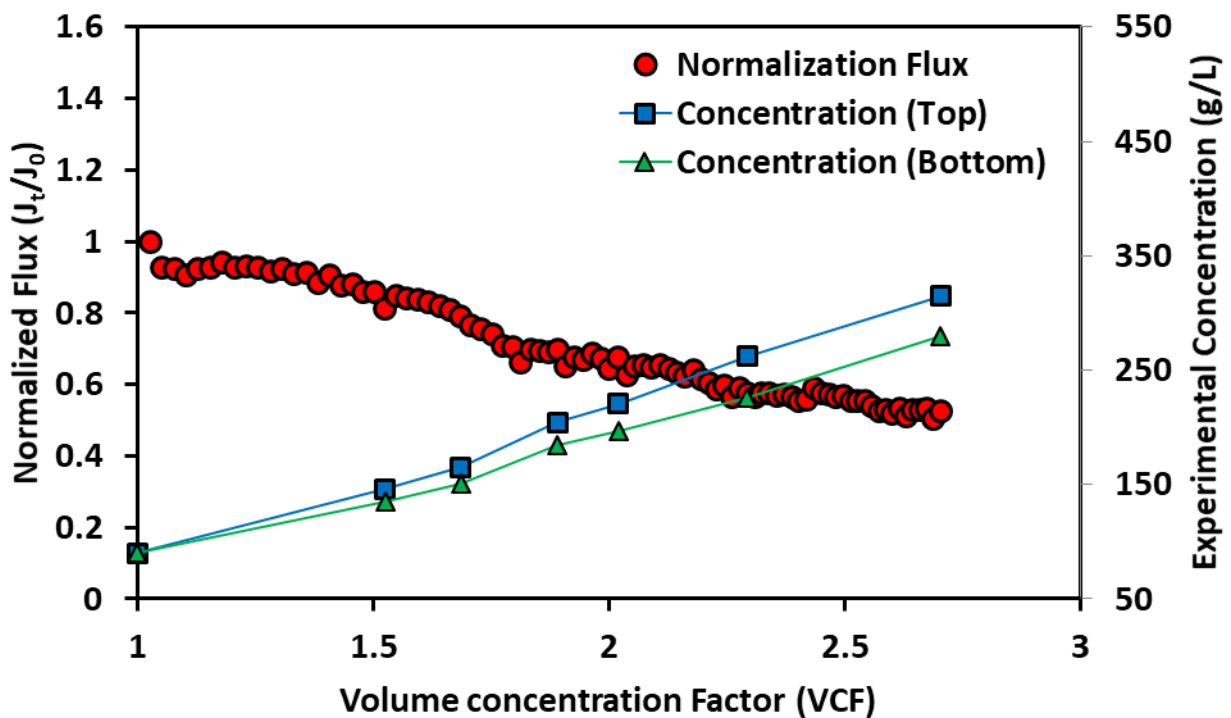
253

254

255

The F-SMDC was carried out using S-DCMD configuration. The feasibility of different submerged MD configurations (submerged vacuum direct contact MD called as S-VDCMD) in F-SMDC process was examined under the same operational condition. The motivation for using S-VDCMD is the potential of achieving higher permeate flux. In line with this, S-VDCMD achieved a 25% higher initial permeate flux than S-DCMD. However, the CG in F-SMDC with S-VDCMD configuration was not observed. Higher flux decline was also observed with S-VDCMD compared to F-SMDC with S-DCMD configuration (**Figure 7**) with slightly lower feed concentration at the bottom portion than at the top portion of the reactor. This was attributed to the application of vacuum. In a previous S-MD study [3], it was found that the deposition and adhesion of crystals on the membrane surface was intensified by the presence of vacuum pressure in the MD, resulting in more prevalent fouling. In S-VDCMD, concentrated ions were captured in the membrane boundary

256 layer due to stronger driving force (vacuum pressure) compared to S-DCMD [3]. This restricted the
 257 movement of concentrated feed solution, and it stagnated close to the membrane surface. The
 258 increase in diffusion potential of concentrated feed solution at the top portion rather than the
 259 precipitation downward, resulted in the formation of higher concentration at the top portion than the
 260 bottom portion of the reactor. The results highlighted that S-MD using vacuum was not suitable for
 261 F-SMDC process.



262

263 **Figure 7** Normalized flux and concentration tendency in F-SMDC comparing with S-VDCMD.

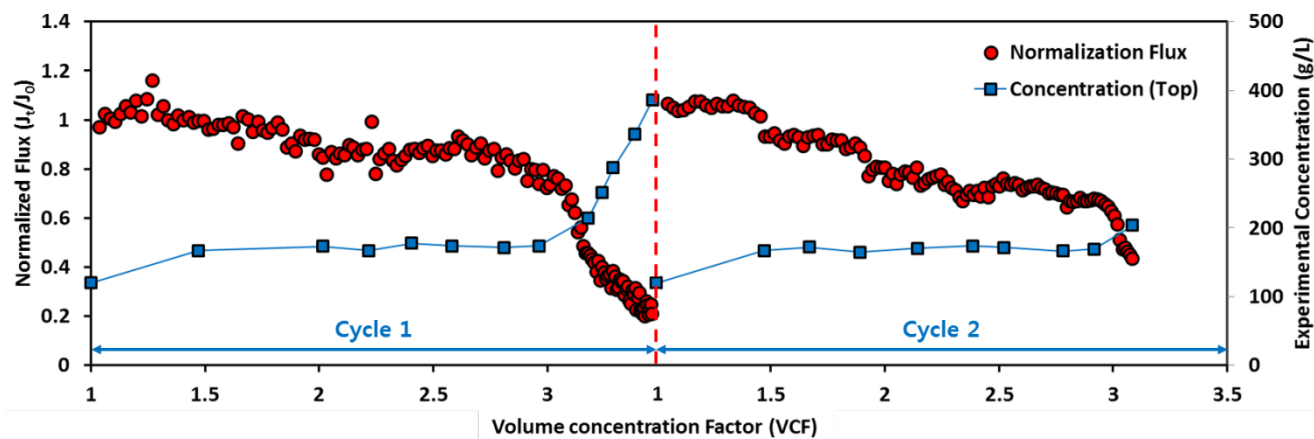
264

265 4.2. Continuous F-SMDC operation

266 The stability of F-SMDC in treating high concentration solution was examined by carrying
 267 out two repeated cycles of operation using the same membrane. At the end of each cycle, used
 268 membrane was submerged in DI water and stirred at 200 rpm for 10 mins to rinse/clean the
 269 membrane before the subsequent operation.

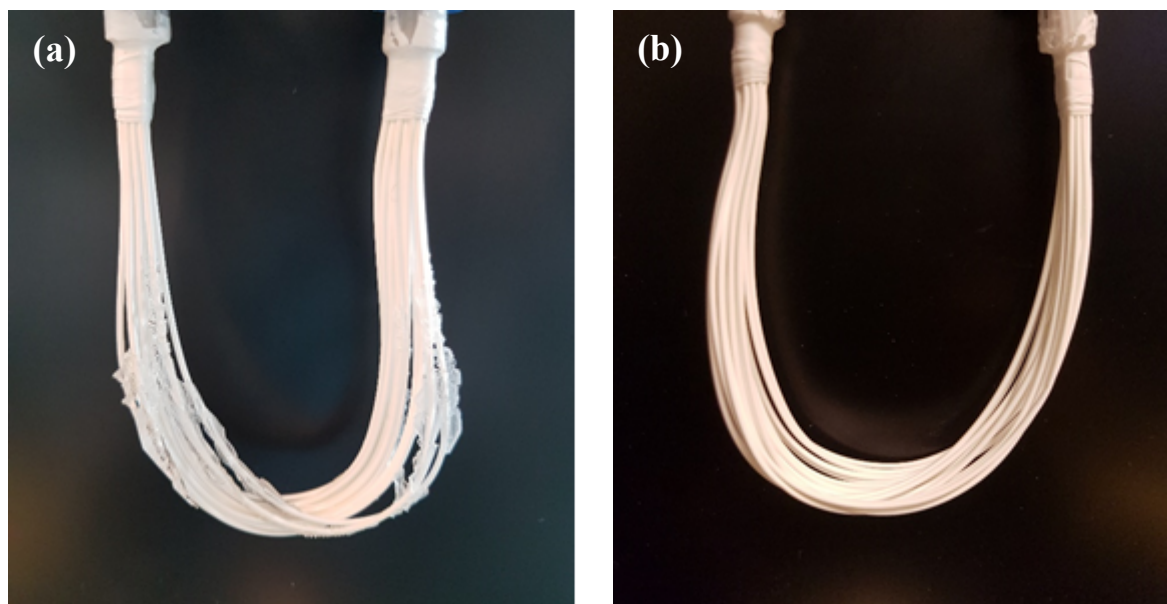
270 In S-DCMD configuration, generally, the membrane surface feed temperature is lower
271 compared to bulk feed temperature due to direct contact with cold permeate on the membrane
272 surface. This factor plays a prevalent role in the solubility of certain crystal salts that are especially
273 influenced by the effect of temperature. One such salt is Na_2SO_4 , which exhibits lower solubility at
274 low temperature (91 g/L @ 10 °C, and 195 g/L @ 20 °C) and higher solubility at increased
275 temperature (488 g/L @ 40 °C). This characteristic of Na_2SO_4 can lead to higher saturation state on
276 the membrane surface, and aggravate the formation of crystals. This results in the non-continuity of
277 MDC process.

278 The effect of this phenomenon can be mitigated in F-SMDC by creating and maintaining CG
279 in the reactor. The feed concentration (under 195 g/L) was lower at the top portion of the reactor
280 which contains the submerged membrane. Here, the direct contact with the permeate solution
281 (16.5 ± 0.2 °C) lowered the feed solution temperature which was set at 50.0 ± 1.3 °C. Specifically, the
282 feed concentration at the top portion of the reactor was maintained at 171.8 ± 5.1 g/L in cycle 1 and
283 169.2 ± 3.0 g/L in cycle 2. At these concentration ranges of Na_2SO_4 , super-saturation was not reached
284 at 16.5 ± 0.2 °C (feed temperature at bottom portion). As such, salt precipitation followed by crystal
285 deposition on the membrane surface was delayed up to around VCF 3.0 as shown in **Figure 8**. In
286 both cycles 1 and 2, fouling on the membrane surface was not detected due to the lower
287 concentration at the top portion. However, in cycle 1, the fouling phenomenon on the membrane
288 surface was detected after VCF 3.0 (**Figure 9**). This was due to rapid increase of concentration
289 (214.4 to 385.5 g/L) upon reaching VCF 3.0. Rapid flux decline occurred beyond this point (**Figure**
290 **8**).



291

292 **Figure 8** Flux and concentration variation in continuous F-SMDC (without crystal extraction until the
 293 completion of each cycle).



294 **Figure 9** Used membrane with Na_2SO_4 treatment at the end of (a) cycle 1, (b) cycle 2.

295

296 Initial crystal formation at the bottom portion of the reactor occurred at around VCF 2.2 in
 297 both cycles. At VCF 2.8 and above, the bottom portion of the reactor was completely filled with
 298 crystals. At this point, the feed concentration at the top portion of the reactor increased rapidly, and
 299 CG in the F-SMDC feed reactor was no longer maintained. As such, it is essential to continuously

300 extract crystals generated at the bottom portion of the reactor to maintain a feed concentration
301 gradient in the F-SMDC process. For this reason, an external crystallizer was used in this study as
302 described in section 2.1.

303 At the end of each operation cycle, Na₂SO₄ solution remained at the top and middle portions
304 of the reactor. It must be highlighted that the F-SMDC was carried out in a batch mode. In the
305 scenario of a continuous mode operation, periodic crystal extraction from the bottom portion of the
306 reactor would be possible. This would enable continuous crystal growth simultaneously, while
307 achieving near zero liquid discharge in the reactor. However, in view of the batch mode operation of
308 this study, an external crystallization was used to evaluate the potential of further crystal growth with
309 the remaining Na₂SO₄ solution. This would enable to depict the near zero liquid discharge scenario
310 of a continuous mode. In depth evaluation of F-SMDC operation in a continuous mode will be
311 explored in future studies to establish this scenario.

312 Upon allowing the reactor to stand at room temperature (23.2±0.3 °C) for 3 days (72 h),
313 further salt crystallization occurred due to its super-saturated state (**Table 2**). This step enabled the
314 generation of additional crystals, thereby, increasing the total amount of crystals. Although the initial
315 concentrations in both cycles were different (because of different degree of concentrate: VCF 3.5 in
316 cycle 1 vs. VCF 3.0 in cycle 2), the final concentrations of both cycles were similar. However, the
317 solution volume reduction ratio varied (87% in cycle 1 vs. 47% in cycle 2) (**Table 2**). The simple
318 step of allowing the feed solution to remain at room temperature without additional treatment
319 enabled to decrease the feed concentration and volume by 32% and 46% respectively. Further, the
320 small quantity of remaining solution at the top and middle portions of the reactor can be channelled
321 back to the bulk feed tank for a subsequent F-SMDC operation cycle. This indicated that F-SMDC
322 with external crystallization does have the potential to achieve near zero liquid discharge.

323 **Table 2** Volume and concentration of feed solution extracted from reactor upon F-SMDC and upon
 324 external crystallization (standing at room temperature for 24 - 72 h).

Sample	1 st cycle		2 nd cycle	
	Concentration (g/L)	Amount (mL)	Concentration (g/L)	Amount (mL)
Final F-SMDC feed (Before crystallization)	329.4±6.1	1140	218.1±2.3	1160
Upon external crystallization	160.4±0.2 (24 h)	150	160.4±0.7 (24 h)	620
	149.9±2.3 (72 h)		147±0.3 (72 h)	

325

326 4.3. Crystal production in F-SMDC

327 In F-SMDC, crystals were generated at the bottom portion of the reactor due to high
 328 concentration and lower temperature setting. In this study, the bottom portion of the reactor was
 329 cooled down up to 20.0±0.5 °C while the top portion of the reactor was maintained at 50.0±1.3 °C.
 330 At the bottom portion of the reactor, the combined condition of higher feed concentration and lower
 331 temperature enabled to achieve a faster super-saturation state of Na₂SO₄ compared to the top portion
 332 of the reactor. The CG and TG in the F-SMDC (lower concentration and higher temperature at top
 333 portion, higher concentration and lower temperature at bottom portion) improved the efficiency of
 334 recovering valuable crystals as well as obtaining higher water recovery and better stability (lower
 335 scaling) of MD process.

336 When 120 g/L Na₂SO₄ was treated without using crystals extraction, crystals were generated
 337 both at the top and bottom portions of the reactor. The amount of generated crystals formed was

338 directly proportional to the concentration ratio of feed solution (**Table 3**). High amount of crystals
 339 was generated both during cycle 1 (1169.0 g) and cycle 2 (898.0 g). In the case of cycle 1, F-SMDC
 340 operation was carried on beyond the point of rapid flux decline in order to obtain a highly
 341 concentrated final solution. The rapid permeate flux decline due to fouling and high feed
 342 concentration degraded the stability of the process. Therefore, it is not recommended to operate F-
 343 SMDC beyond the super-saturation state of the feed solution in the future study.

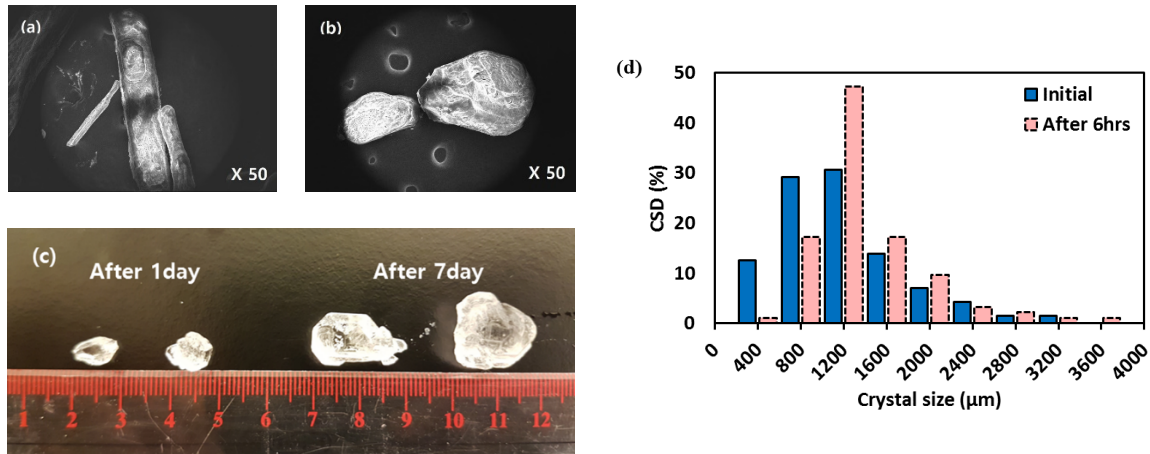
344 **Table 3** Crystal and fresh water production by F-SMDC operation (feed: Na₂SO₄).

Sources	1 st cycle		2 nd cycle	
	Produced crystal (g)	Produced fresh water (mL)	Produced crystal (g)	Produced fresh water (mL)
Bottom portion of the reactor	551.3		541.6	
External crystallizer (containing saturated solution from top and middle portion of the reactor)	617.7	4295.5 (99% ion rejection)	356.4	3561.4 (99% ion rejection)
Total	1169.0		898.0	

345

346 The crystal production rate can be increased by factors such as temperature control, crystal
 347 size and immersion of crystals into saturated solution. As shown in **Table 2**, the volume and
 348 concentration of mother liquid decreased due to the formation of Na₂SO₄ crystals with time. For
 349 instance, the feed concentration of 160.4±0.2 g/L after 24 h was reduced to 149.9±2.3 g/L after 72 h.
 350 This indicated that additional crystals of larger sizes can be produced by the immersion of initial
 351 crystals into the mother liquid (**Figure 10(d)**). The morphology of Na₂SO₄ crystals changed from

352 rectangle shape to spherical shape over time (**Figure 10(a), (b) and (c)**). Prevalent growth and
 353 change in shape of crystals were detected on crystals that were fully immersed in the mother liquid.
 354 The results indicated that direct contact with mother liquid would enhance the growth of crystals. It
 355 is therefore essential to have enough contact area and immersion time with mother liquid. By doing
 356 so, a narrow size distribution of the crystals can be obtained.



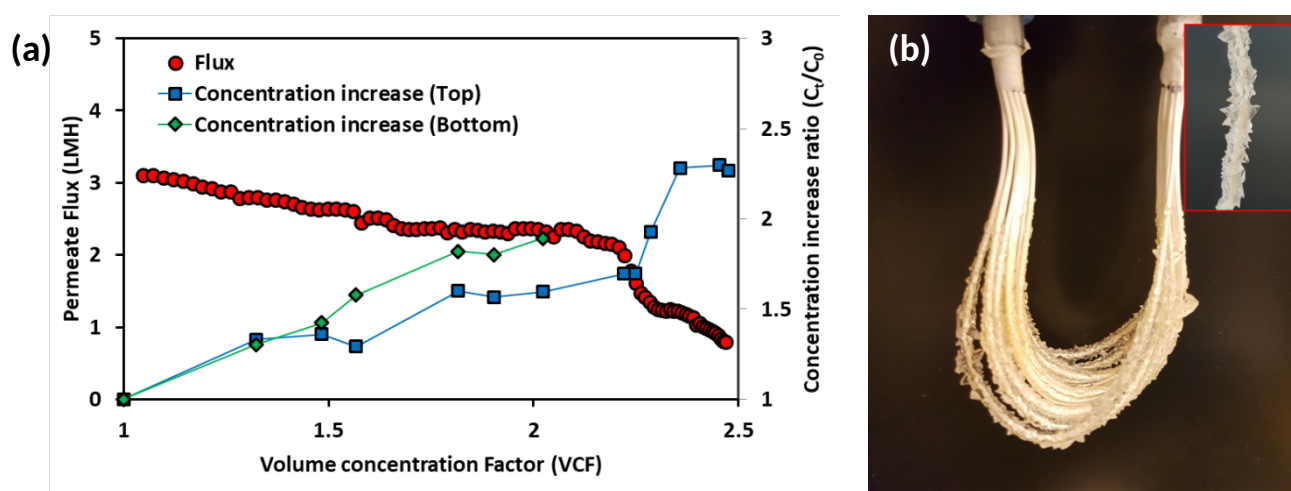
357 **Figure 10** Crystal size distribution (CSD) and change in morphology of produced Na_2SO_4 crystals with
 358 time. Images of crystals at (a) initial, and after (b) 60min and (c) 1 day and 7 days, and (d) size distribution of
 359 Na_2SO_4 .

360

361 4.4. Effect of salinity

362 The effect of salinity in the treatment of Na_2SO_4 solution was examined by adding NaCl. As
 363 shown in **Figure 11**, the concentration gradient trend at the initial stage (up to VCF 1.5) was similar
 364 with and without the presence of NaCl. In the presence of NaCl, the formation of crystals at the
 365 bottom portion of the reactor started from around VCF 1.8, while the concentration at the top portion
 366 of the reactor increased (with and without the presence of NaCl), lower VCF was achieved in the
 367 presence of NaCl. In the presence of NaCl, from VCF 2.2 onwards, visible presence of crystals was
 368 observed. At the same time, rapid flux decline and increase of feed concentration at the top portion

369 of the reactor occurred. This occurrence was associated to the presence of crystals on the membrane
 370 surface. The F-SMDC operation condition, namely concentrated feed solution and cooler membrane
 371 surface condition (direct contact with cold permeate) enabled the generation of CG. The crystal
 372 deposition on the membrane surface reduced the effective membrane area. This decreased the rate of
 373 concentration and degree of cooling by permeate, resulting in reduced crystallization of concentrated
 374 solution. Therefore, concentrated solution remained at the vicinity of the membrane boundary layer,
 375 and feed concentration at the top portion of the reactor portion increased by diffusion. This caused an
 376 increased crystal deposition onto the membrane surface (**Figure 11 (b)**).



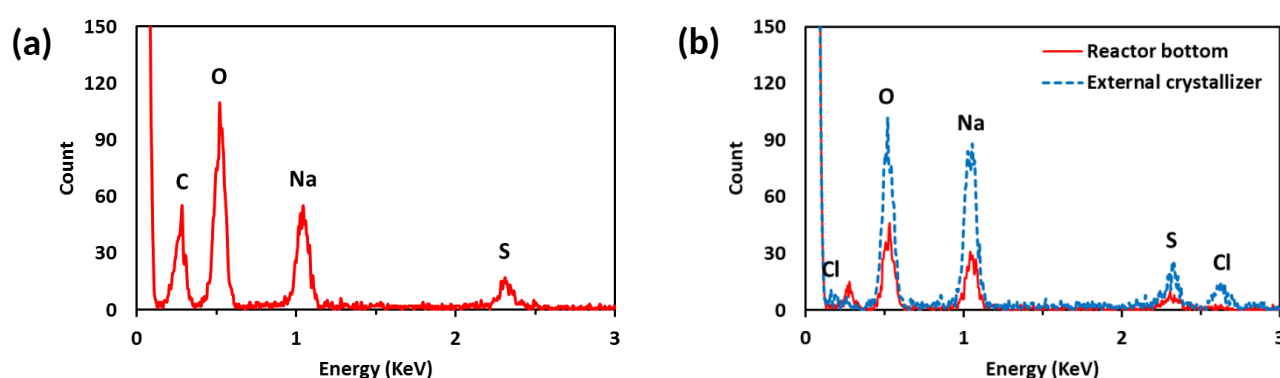
377 **Figure 11** F-SMDC with Na_2SO_4 and NaCl : (a) variation of flux and concentration at the top and bottom
 378 portion of the reactor, (b) used membrane at the end of the experiment.

379

380 The EDX analysis revealed the presence of sodium, oxygen and sulphur elements on the used
 381 membrane surface and at the bottom portion of the reactor (**Figure 12(a)** and **(b)**). On the other hand,
 382 chloride ion was detected in crystals generated in feed solution of the top and middle portions of the
 383 reactor. The results indicated that a separate generation of crystal from solution can be achieved by a
 384 control of concentration and temperature at suitable range. In addition, the concentration of sodium
 385 ion in solution seems to influence crystallization phenomenon on the membrane surface and at the

386 bottom portion of the reactor. The crystallization on the membrane surface was detected at around
387 VCF 3.3 in the absence of NaCl. The crystals formation on the membrane surface became faster
388 (around VCF 2.2) with NaCl. At this point, the concentrations of sodium ion in both feed solutions
389 with and without NaCl were similar (93.08 g/L without NaCl and 93.28 g/L with NaCl). Also, upon
390 crystal formation at the bottom portion of the reactor, similar amount of sodium ion concentration
391 was observed in both the feed solutions (without NaCl: 107.78 g/L in cycle 1 / 106.26 g/L in cycle 2,
392 and with NaCl: 106.08 g/L). The difference in the initial point of crystallization on the membrane
393 surface and at the bottom of the reactor was attributed to temperature difference.

394



395 **Figure 12** EDX analysis of crystals (a) deposited on the used membrane surface, (b) produced from the
396 bottom portion of the reactor and external crystallizer (saturated feed solution from the top and middle portion
397 of the reactor) (feed solution: Na₂SO₄ and NaCl).

398

399 5. Conclusions

400 The feasibility of fractional submerged membrane distillation-crystallization (F-SMDC)
401 process was evaluated using a feed solution containing high concentration of Na₂SO₄ without and
402 with NaCl. The following conclusions were made from the experimental investigation:

- 403 • F-SMDC setting enabled the creation of CG and TG using a partition and double wall
404 heating/cooling in the feed reactor. A lower feed concentration and higher feed temperature
405 was maintained at the top portion of the reactor. Meanwhile, higher feed concentration and
406 lower feed temperature was maintained at the bottom portion of the reactor.
- 407 • The presence of CG/TG in F-SMDC enabled to achieve higher water recovery (VCF 3.5) and
408 lower membrane scaling, compared to SMDC mode (VCF 2.9).
- 409 • The condition of elevated feed concentration and lower temperature at the bottom portion of
410 the reactor was favourable for high crystal formation in F-SMDC.
- 411 • The presence of salt (NaCl) influenced the crystallization of Na_2SO_4 at the bottom portion of
412 the reactor and on the membrane surface, resulting in higher crystallization in both locations.
- 413 • F-SMDC was effective in reducing membrane scaling, producing high quality fresh water
414 and valuable crystals (Na_2SO_4).
- 415 • The shape and dimension of F-SMDC reactor are essential factors that influence the
416 formation of CG/TG and the overall F-SMCD performance. Further optimization of the
417 reactor configuration is an important factor that must be explored in detail.

418

419 **Acknowledgement**

420 This work was funded by Australian Research Council Discovery Research Grant (DP150101377)
421 and two Basic Science Research Programs through the National Research Foundation of Korea
422 (NRF) funded by the Ministry of Education (2017R1A6A3A04004335) and the Ministry of Science,
423 ICT, & Future Planning (2017R1A2B3009675).

425 **References**

- 426 [1] L.A. Hoover, W.A. Phillip, A. Tiraferri, N.Y. Yip, M. Elimelech, Forward with osmosis: Emerging
427 applications for greater sustainability, *Environmental Science and Technology*, 45 (2011) 9824-9830.
- 428 [2] J. Cebrian, C.M. Duarte, Detrital stocks and dynamics of the seagrass *Posidonia oceanica* (L.) Delile in the
429 Spanish Mediterranean, *Aquatic Botany*, 70 (2001) 295-309.
- 430 [3] Y. Choi, G. Naidu, S. Jeong, S. Vigneswaran, S. Lee, R. Wang, A.G. Fane, Experimental comparison of
431 submerged membrane distillation configurations for concentrated brine treatment, *Desalination*, 420 (2017)
432 54-62.
- 433 [4] X. Ji, E. Curcio, S. Al Obaidani, G. Di Profio, E. Fontananova, E. Drioli, Membrane distillation-
434 crystallization of seawater reverse osmosis brines, *Separation and Purification Technology*, 71 (2010) 76-82.
- 435 [5] G. Naidu, S. Jeong, Y. Choi, S. Vigneswaran, Membrane distillation for wastewater reverse osmosis
436 concentrate treatment with water reuse potential, *Journal of Membrane Science*, 524 (2017) 565-575.
- 437 [6] Y. Choi, G. Naidu, S. Jeong, S. Lee, S. Vigneswaran, Effect of chemical and physical factors on the
438 crystallization of calcium sulfate in seawater reverse osmosis brine, *Desalination*, 426 (2018) 78-87.
- 439 [7] G. Naidu, S. Jeong, Y. Choi, M.H. Song, U. Oyunchuluun, S. Vigneswaran, Valuable rubidium extraction
440 from potassium reduced seawater brine, *Journal of Cleaner Production*, 174 (2018) 1079-1088.
- 441 [8] S. Jeong, G. Naidu, R. Vollprecht, T. Leiknes, S. Vigneswaran, In-depth analyses of organic matters in a
442 full-scale seawater desalination plant and an autopsy of reverse osmosis membrane, *Separation and*
443 *Purification Technology*, 162 (2016) 171-179.
- 444 [9] D. Squire, Reverse osmosis concentrate disposal in the UK, *Desalination*, 132 (2000) 47-54.
- 445 [10] D. Squire, J. Murrer, P. Holden, C. Fitzpatrick, Disposal of reverse osmosis membrane concentrate,
446 *Desalination*, 108 (1997) 143-147.

- 447 [11] J.S. Ho, Z. Ma, J. Qin, S.H. Sim, C.-S. Toh, Inline coagulation–ultrafiltration as the pretreatment for
448 reverse osmosis brine treatment and recovery, *Desalination*, 365 (2015) 242-249.
- 449 [12] P. Loganathan, G. Naidu, S. Vigneswaran, Mining valuable minerals from seawater: a critical review,
450 *Environmental Science: Water Research & Technology*, 3 (2017) 37-53.
- 451 [13] G. Naidu, S. Jeong, M.A.H. Johir, A.G. Fane, J. Kandasamy, S. Vigneswaran, Rubidium extraction from
452 seawater brine by an integrated membrane distillation-selective sorption system, *Water Research*, 123 (2017)
453 321-331.
- 454 [14] H. Julian, S. Meng, H. Li, Y. Ye, V. Chen, Effect of operation parameters on the mass transfer and
455 fouling in submerged vacuum membrane distillation crystallization (VMDC) for inland brine water treatment,
456 *Journal of Membrane Science*, 520 (2016) 679-692.
- 457 [15] F. Edwie, T.-S. Chung, Development of simultaneous membrane distillation–crystallization (SMDC)
458 technology for treatment of saturated brine, *Chemical Engineering Science*, 98 (2013) 160-172.
- 459 [16] S. Meng, Y. Ye, J. Mansouri, V. Chen, Crystallization behavior of salts during membrane distillation
460 with hydrophobic and superhydrophobic capillary membranes, *Journal of Membrane Science*, 473 (2015)
461 165-176.
- 462 [17] C.M. Tun, A.G. Fane, J.T. Matheickal, R. Sheikholeslami, Membrane distillation crystallization of
463 concentrated salts—flux and crystal formation, *Journal of Membrane Science*, 257 (2005) 144-155.
- 464 [18] F. Macedonio, E. Drioli, Hydrophobic membranes for salts recovery from desalination plants,
465 *Desalination and Water Treatment*, 18 (2010) 224-234.
- 466 [19] C.A. Quist-Jensen, F. Macedonio, D. Horbez, E. Drioli, Reclamation of sodium sulfate from industrial
467 wastewater by using membrane distillation and membrane crystallization, *Desalination*, 401 (2017) 112-119.

- 468 [20] G. Naidu, W.G. Shim, S. Jeong, Y. Choi, N. Ghaffour, S. Vigneswaran, Transport phenomena and
469 fouling in vacuum enhanced direct contact membrane distillation: Experimental and modelling, Separation
470 and Purification Technology, 172 (2017) 285-295.
- 471 [21] A. Alkudhiri, N. Darwish, N. Hilal, Membrane distillation: A comprehensive review, Desalination, 287
472 (2012) 2-18.
- 473 [22] A. Ali, F. Macedonio, E. Drioli, S. Aljlil, O.A. Alharbi, Experimental and theoretical evaluation of
474 temperature polarization phenomenon in direct contact membrane distillation, Chemical Engineering Research
475 and Design, 91 (2013) 1966-1977.
- 476 [23] H. Lu, J. Wang, T. Wang, N. Wang, Y. Bao, H. Hao, Crystallization techniques in wastewater treatment:
477 An overview of applications, Chemosphere, 173 (2017) 474-484.
- 478 [24] S. Meng, Y.-C. Hsu, Y. Ye, V. Chen, Submerged membrane distillation for inland desalination
479 applications, Desalination, 361 (2015) 72-80.
- 480 [25] L. Francis, N. Ghaffour, A.S. Al-Saadi, G.L. Amy, Submerged membrane distillation for seawater
481 desalination, Desalination and Water Treatment, 55 (2015) 2741-2746.
- 482 [26] F. Edwie, T.-S. Chung, Development of hollow fiber membranes for water and salt recovery from highly
483 concentrated brine via direct contact membrane distillation and crystallization, Journal of Membrane Science,
484 421-422 (2012) 111-123.
- 485 [27] Y. Shin, J. Sohn, Mechanisms for scale formation in simultaneous membrane distillation crystallization:
486 Effect of flow rate, Journal of Industrial and Engineering Chemistry, 35 (2016) 318-324.
- 487 [28] L.D. Tijging, Y.C. Woo, J.-S. Choi, S. Lee, S.-H. Kim, H.K. Shon, Fouling and its control in membrane
488 distillation—A review, Journal of Membrane Science, 475 (2015) 215-244.
- 489 [29] S. Goh, J. Zhang, Y. Liu, A.G. Fane, Fouling and wetting in membrane distillation (MD) and MD-
490 bioreactor (MDBR) for wastewater reclamation, Desalination, 323 (2013) 39-47.

491 [30] Y. Choi, S. Vigneswaran, S. Lee, Evaluation of fouling potential and power density in pressure retarded
492 osmosis (PRO) by fouling index, *Desalination*, 389 (2016) 215-223.